Copy 6
RM L51A19

NACA RM L51A19

NACA

RESEARCH MEMORANDUM

FOR REFERENCE

THE TORSIONAL DEFLECTIONS OF SEVERAL PROPELLERS UNDER OPERATING CONDITIONS

By W. H. Gray and A. E. Allis

Langley Aeronautical Laboratory
Langley Field, Va.

NATIONAL ADVISORY COMMITTEE
FOR AERONAUTICS

WASHINGTON

June 22, 1951

NATIONAL ADVISORY COMMITTEE FOR AERONAUTICS

RESEARCH MEMORANDUM

THE TORSIONAL DEFLECTIONS OF SEVERAL PROPELLERS UNDER OPERATING CONDITIONS

By W. H. Gray and A. E. Allis

SUMMARY

Propeller-blade torsional-deflection data obtained during an investigation of the pressure distribution on constant-chord solid aluminum-alloy blades differing only in camber and thickness are presented herein. Blade-section aerodynamic moments obtained from the measurements of pressure distribution have been used to compute the blade torsional deflections, and the measured and computed results are compared.

The magnitude of blade torsional deflection was not negligible and varied with blade design; the thinner the blade, the greater the deflection. The deflections could be computed with good accuracy from a knowledge of the section physical characteristics, the aerodynamic forces acting on the blade, and propeller operating conditions.

This work indicates that blade torsional deflection should be considered especially in the design of thin propeller blades. A large effect on power coefficient was encountered for a condition at which the effect on efficiency was small.

INTRODUCTION

The constant effort to maintain good propeller efficiency even at high subsonic flight speeds has resulted in the use of very thin propeller blade sections. Thin sections, however, reduce the ability of a blade to resist torsional deflection and, consequently, greater importance must now be attached to torsional deflection.

Previous optical measurements of blade torsional deflection under operating conditions, such as presented in reference 1, indicated negligible torsional deflections. The blades used in these earlier investigations, however, were considerably thicker than are now considered desirable. Prior to the present research a theory also existed for the

calculation of blade deflections of propellers operating with combined lift and centrifugal forces, but no extensive comparison of measured and calculated data had been made.

The present trend in the design of efficient propellers is in the direction to increase the importance of blade twist. Unless attention is given to designing for a condition of no twist by the arduous process of selecting sections having the proper aerodynamic as well as geometric characteristics, thin propellers operating at high speeds will experience large values of blade twist. Consequently, the effect of twist may have an important bearing on the expected performance of a propeller.

The purpose of the present investigation was to determine by experiment and by theory the magnitude of blade deflection. This determination of blade torsional deflection was a necessary contribution to the evaluation of the results of a pressure-distribution investigation in the Langley 16-foot high-speed tunnel. Experimental values of blade torsional deflections were obtained concurrently with the pressure-distribution data. The investigation was therefore comprehensive.

A desirable consideration in the present investigation is to show the possible application of the propeller-deflection theory in the propeller design stage as it is conceivable that torsional deflections may influence blade design.

SYMBOLS

b	blade chord, feet
c_l	blade-section lift coefficient
c_{l_d}	blade-section design lift coefficient
c_m	section pitching-moment coefficient about quarter-chord point
c_n	section normal-force coefficient
D	propeller diameter, feet
G	shear modulus of elasticity, pounds per square foot
h	blade-section maximum thickness, feet

[redacted]

I_p	polar moment of inertia, feet^4
I_x	moment of inertia about axis through center of gravity parallel to chord line, feet^4
I_y	moment of inertia about axis through center of gravity perpendicular to chord line, feet^4
J	advance ratio (V/nD)
J'	torsional stiffness constant, feet^4
M	Mach number of advance
M_a	aerodynamic torsional moment, foot-pounds
M_c	tensile torsional moment, foot-pounds
M_p	planipetal torsional moment, foot-pounds
M_x	helical section Mach number $\left(M\sqrt{1 + \left(\frac{\pi x}{J}\right)^2}\right)$
N	propeller rotational speed, revolutions per minute
n	propeller rotational speed, revolutions per second
q_x	resultant dynamic pressure at a radial station x, pounds per square foot $\left(1/2\rho W_o^2\right)$
R	propeller-tip radius, feet
r	radius to a blade element, feet
s	distance from leading edge to any point on chord, feet
$\bar{s}$	distance from leading edge to flexural center of section, feet
σ	centrifugal stress, pounds per square foot
t	section thickness perpendicular to the camber line, feet
V	velocity of advance (corrected for wind-tunnel wall-interference effects), feet per second

[redacted]

W_o	resultant section velocity vector, feet per second $\left(V\sqrt{1 + \left(\frac{\pi x}{J}\right)^2}\right)$
W	resultant velocity at blade section, feet per second
w_i	induced velocity at blade section, feet per second
x	fraction of propeller-tip radius (r/R); also used as a subscript to denote any section
α	angle of attack of blade element, corrected for induced flow and blade deflection, at radial station x, degrees $(\beta - \phi + \Delta\beta)$
α'	geometric angle of attack of blade element at radial station x, degrees $(\beta - \phi_o)$
α_i	induced angle of attack, degrees
β	static blade angle, degrees
$\beta_{0.75R}$	static blade angle at 0.75 tip radius, degrees
$\Delta\beta$, θ	blade torsional deflection or blade twist, degrees
λ	inclination of sighting station to vertical, degrees
ρ	mass density of air in free stream, slugs per cubic foot
ρ_m	mass density of blade material, slugs per cubic foot
ϕ	aerodynamic helix angle, degrees
ϕ_o	geometric helix angle, degrees $\left(\tan^{-1} (J/\pi x)\right)$
ω	angular velocity, radians per second

DESCRIPTION OF APPARATUS

General.- An investigation was made of the torsional deflections on the blade sections of four two-blade constant-chord solid aluminum-alloy propellers which differed only in thickness or section camber.

[redacted]

The investigation was conducted in the Langley 16-foot high-speed tunnel on the 2000-horsepower dynamometer which is described fully in reference 2.

Propellers.- The propellers investigated are identified by Roman numerals and are designated by their blade design numbers as follows:

I	NACA 10-(3)(049)-03
II	NACA 10-(0)(066)-03
III	NACA 10-(5)(066)-03
IV	NACA 10-(3)(090)-03

Using the NACA 10-(3)(049)-03 propeller as an example, the digits in the first group of numbers indicate a nominal 10-foot-diameter propeller with the following design parameters at the 0.7 radius: section design lift coefficient of 0.3, thickness ratio of 0.049, and solidity of 0.03 per blade. The NACA 16-series blade sections are used in all four propellers, each propeller having a constant value of design lift coefficient along the radius to $x = 0.95$. Blade-form curves are shown in figure 1 and values of section blade angle for all propellers are given in table I. In the subsequent discussion of the propeller blades the Roman numeral designation will be used. One blade of each propeller contained tubes which were installed for the pressure-distribution investigation as reported in references 3 to 6.

Optical deflectometer.- The optical deflectometer was employed during the torsional-deflection investigation of each one of these four blade designs and is described in the appendix.

Mirrors.- The small, rhodium-coated, first surface reflecting mirrors were fixed to the thrust face of the untubed blade for each propeller at three radial stations, $x = 0.45$, 0.70, and 0.90 (fig. 2). The hard rhodium surface proved most satisfactory because of its ability to maintain a good reflecting surface after continuous propeller operation. The reflecting surface was about 5/16 of an inch square, and the mirror thickness was 1/32 of an inch. A combination of mirror sizes and bonding materials was investigated before a positive method of securing the mirror firmly to the blade was achieved. The most satisfactory combination was found to be the mirror size noted above bonded to the blade with a thermopolymeric cement with the mirror edges faired to the blade by plastic metal.

TESTS

Blade torsional deflection, which, for brevity, will hereafter be referred to as blade twist, was measured at three radial stations,

$x = 0.45$, 0.70, and 0.90 for a nominal blade angle setting of 45° at the three-quarter radius (table I). Advance ratio $\left(J = \frac{V}{nD}\right)$ was varied by maintaining the rotational speed constant and varying the tunnel airspeed for some of the runs. The remainder of the runs were made with the tunnel-air-stream Mach number held constant, and a range of advance ratio was investigated by changing the propeller rotational speed. Tests were run from zero torque to full load to facilitate operation of the deflectometer. Starting at zero torque provided two advantages: (1) the dynamometer would not overheat if the deflectometer operator required any length of time to locate the initial test point and (2) the deflections were normally small at zero torque and therefore little movement of the deflectometer was required to locate the initial point.

REDUCTION OF DATA AND ACCURACY

Because of the restriction to the normal flow through the propeller caused by the presence of the wind-tunnel walls, the usual wind-tunnel-wall corrections as described in reference 2 have been applied to the data to obtain the equivalent free-stream airspeed.

It is believed that blade twist was measured within 0.10° as the majority of the faired repeat runs agree within this accuracy. Figure 3 shows two sets of typical blade-twist data recorded at the $x = 0.90$ station for propeller II operating at 1600 rpm.

Sources of error associated with the technique employed are: (1) the blade twist was measured on the blade without pressure tubes, whereas the calculations are based on data from the blade with pressure tubes; (2) the tunnel vibration was high, especially on the constant Mach number runs, and it was necessary for the deflectometer operator to average the reflected images.

The most desirable method of measuring blade twist would have been to record simultaneously the twist values for the three stations investigated. It would also have been desirable to obtain the pressure-distribution measurements simultaneously at all nine stations. Neither of these two conditions was feasible. When correlation of these non-simultaneous groups of runs in order to compare measured and computed data was attempted, some differences in velocity or Mach number were present.

BLADE-TWIST THEORY AND COMPUTING PROCEDURE

A general discussion of the large amount of data presented for the four propellers requires that a brief résumé of the various factors which contribute to twist, as well as the method of computation of the twist, be presented. The theory used herein in calculating blade twist is essentially the same as presented in reference 7.

Three moments are considered to act on a rotating propeller blade to produce twisting: aerodynamic torsional moment M_a, planipetal torsional moment M_p, and tensile torsional moment M_c. Blade twist at a given radius r is then equal to

$$\frac{180}{\pi}\int_0^r \frac{M_a + M_p' + M_c}{GJ'}\,dr$$

The aerodynamic moment can be positive or negative and therefore can act in a direction to increase or decrease blade twist. The position of the center of pressure and the magnitude and sign of the normal-force coefficient are the principal factors entering into the magnitude and direction of twist of the aerodynamic moment. The basic equation used in calculating this moment at station x is

$$M_{a_x} = R\int_x^{1.00} q_x b^2 \left[\left(\bar{s} - \frac{b}{4}\right)\frac{c_n}{b} + c_m\right] dx \qquad (1)$$

As may be seen from this equation, the magnitude and direction of twist of the aerodynamic moment are directly affected by the location of the flexural center. By definition, the flexural center of a section of a beam is that point in the section plane through which a transverse load must act if bending deflection only is to be produced with no twist of the section. An approximate formula for the location of the flexural center of an airfoil section is given in reference 8. For thin sections having small camber where the chord line may be considered as the median line,

$$\bar{s} = \frac{\int_0^b t^3 s\,ds}{\int_0^b t^3\,ds}$$

[redacted]

The flexural axis of the blade would then be considered to be the loci of all such points along the blade. Normally it is most convenient and sufficiently accurate to assume that the center of gravity coincides with the flexural center of an airfoil section. For the case of the 16-series sections, the flexural center and the center of gravity are located at s = 0.48b, and equation (1) reduces to the form

$$M_{a_x} = R\int_x^{1.00} q_x b^2 (0.23\, c_n + c_m)\,dx \tag{1a}$$

which was used for the computed data presented herein.

The planipetal moment at each section is produced by a component of centrifugal force acting in a plane normal to the flexural axis. This moment tends to decrease the section blade angle under all operating conditions and its value at any station is expressed by the equation

$$M_{p_x} = -\frac{\omega^2 \rho_m R}{2}\int_{x_{\text{hub}}}^{1.00} \sin 2\beta (I_y - I_x)\,dx \tag{2}$$

The centrifugal untwisting moment is analogous to an end pull on the blade. It tends to remove the twist from the blade and its value at any station is given by

$I_{p_x} = I_{xx} + I_{yy}$

$$M_{c_x} = \frac{\pi}{180}\left[I_{p_x}\sigma_x\left(\frac{d\beta}{dr}\right)_x\right] \tag{3}$$

Unlike the other two moments, the centrifugal untwisting moment is not integrated along the blade.

The ability of the section to resist the twisting moments is determined by the product of the factors G and J'. The shear modulus of elasticity G is a characteristic of the material of which the blade is constructed, and the torsional stiffness constant J' is a shape parameter. The latter may be determined experimentally or computed by an approximate formula (references 7 and 8). An approximate formula given in reference 8 that applies to an airfoil section indicates that J' varies as the third power of the blade thickness and linearly with blade chord as follows:

$$J' = \frac{1}{3}\int_0^b t^3\,ds$$

[redacted]

Section values of stiffness constant were calculated for the propellers investigated and were used in computing blade twist. A static bench test revealed that for a given applied moment the measured blade twist was in close agreement with a calculated twist obtained by using calculated values of section stiffness constant. Further static tests revealed that the difference in measured values of blade twist for propellers having the same thickness ratio and different cambers was found to be negligible. Figure 4 shows the good agreement between static measured values and calculated values of blade twist for two propellers differing only in camber. It was also ascertained by static bench tests that there was a negligible difference in measured values of blade twist between blades mounting mirrors (which contained no pressure tubes) and those containing tubes.

A value of G of 4.1×10^6 pounds per square inch (5.9×10^8 lb/sq ft) has been assumed for the shear modulus of elasticity of aluminum alloy in these computations.

A procedure for computing twist.- Blade twist was computed for propellers for which the section pressure distributions were available and therefore the problem of computing the aerodynamic twisting moment was relatively simple. First c_n and c_m were evaluated from the pressure distributions for a common parameter, J, for all test conditions at which the aerodynamic twisting moment was desired. A sufficient number of radial stations were investigated so that the radial distribution of c_n and c_m was established. The value of the incremental aerodynamic moment was computed and the final value of the aerodynamic twisting moment at any station was then the sum of the incremental moments outboard of that station. Because pressure-distribution data obtained from a rotating propeller were used, it was not necessary to perform a series of successive approximations to find the aerodynamic moment; c_n and c_m were measured after the blade had twisted.

If two-dimensional data are used to compute blade twist, the aerodynamic moment must be determined by a series of approximations. This procedure is necessary because blade twist is assumed equal to zero in the initial computation so that the value of $\alpha = \beta - \phi_o - \alpha_i$. When blade twist is considered, $\alpha = \beta - \phi_o - \alpha_i + \Delta\beta$. The number of successive approximations required are determined by the magnitude of the twist involved as well as the desired accuracy.

The two centrifugal moments M_c and M_p are primarily functions of the blade geometric characteristics and rotational speed. For the usual operating conditions the tensile torsional moment is always opposite in sense to the planipetal torsional moment and for the propellers tested the tensile moment was generally larger. Consequently,

[redacted]

the sum of centrifugal moments tended to increase the section blade angles. For a section operating at a negative blade angle the tensile untwisting moment and the planipetal moment will be additive for that section.

Regardless of the type of aerodynamic data used in the calculations, it is always necessary to perform a series of approximations to both centrifugal moments. The reason for this approach is evident because both expressions for the centrifugal moments contain a term for section blade angle which varies from a static value to a twisted operating value. The number of iterations necessary depends upon the accuracy desired. In the present investigation the second approximation always decreased the absolute value of blade twist from the initial calculation. In general, the correction amounted to 5 to 10 percent of the original calculated value of blade twist.

For any given operating condition, the three moments which contributed to blade twist are summed and equated to $GJ' \frac{d\theta}{dr}$ where $\frac{d\theta}{dr}$ is the twist per unit blade length. The total torsional deflection $\Delta\beta$ at any station is then equal to

$$\int_0^r \frac{d\theta}{dr}\,dr = \frac{180}{\pi}\int_0^r \frac{M_a + M_p + M_c}{GJ'}\,dr$$

It has also been tacitly assumed that the available theory includes all necessary factors influencing blade twist and that bending does not influence blade twist.

RESULTS AND DISCUSSION

Torsional Deflections

General comments.- The curves presented in figures 5 to 8 are of calculated and measured values of blade twist and represent cross-faired values in the case of measured data. The spanwise variation of torsional deflection was in general consistent throughout the investigation so that any one station may be selected for discussion. In the discussion that follows all reference to measured data will be at the $x = 0.90$ station unless otherwise specified.

Propeller I.- This propeller, the thinnest of all the propellers investigated, experienced the greatest twist. Both large positive and

negative values of blade twist were measured on this blade as shown in figure 5. The largest positive value of measured blade twist was 2.30° at 1500 rpm for a J of 2.20 and the largest negative value of twist was 2.60° at a Mach number of 0.60 and a J of 2.40. A spread of about 4.0° from the lightly loaded to the heavily loaded condition was measured at 1500 rpm. For some conditions of operation the axial travel of the deflectometer was insufficient to cover the entire advance-ratio range, but the data were extrapolated to cover the same range as the pressure-distribution data. Thin propeller sections with their associated small values of torsional stiffness constants were the principal factors causing large twist.

Propeller II.- This propeller, with symmetrical blade sections, experienced positive twist for the advance-ratio range and test conditions investigated as shown in figure 6. The maximum positive value of twist was 1.84° for 1500 rpm at a J of 1.90. Several check runs verified the condition of very little or no increase of twist with decreasing advance-ratio values at high load. This tapering off of blade twist with decreasing advance-ratio values was especially noticeable at 1350 and 1500 rpm. Analysis of the pressure-distribution data indicated that radical changes in normal force and/or pitching moment occurred simultaneously with these deflection changes. These radical changes became evident for stations outboard of $x = 0.7$ which would have the most influence on the integrated blade twist. For instance, at $x = 0.78$ and a rotational speed of 1500 rpm in the range $J = 2.40$ to $J = 1.90$ a decrement of 0.05 in J resulted in an increment in c_n of 0.063; however, in the J range 1.875 to 1.825 the change in c_n was only 0.013. This phenomenon occurred when the range of section Mach number from station $x = 0.78$ to the tip was from 0.70 to 0.82. Simultaneously with the change in increment of c_n with J, the values of c_m decreased slightly. The same phenomenon occurred at a rotational speed of 1350 rpm but was less pronounced than at 1500 rpm. The net effect on twisting moment of the foregoing changes in c_n and c_m is apparent from an inspection of equation (1a) for aerodynamic twisting moment.

Propeller III.- Positive and negative values of twist were measured for propeller III (fig. 7) for the constant rotational speed runs. For the constant Mach number runs the measured twist was mostly negative. Maximum positive twist of 1.02° occurred at 1500 rpm for a J of 2.00. A maximum negative twist of 1.50° occurred at a Mach number of 0.65 for a J of 2.40.

Propeller IV.- The values of measured twist for propeller IV, the thickest propeller, are given in figure 8. At 1600 rpm and a J of 1.80 a maximum positive twist of 0.71° was recorded. The small values

of twist for this propeller may be associated with the high values of section stiffness factors it possesses.

Effect of thickness and camber.- Results of the measured deflections for the four propellers investigated indicated that blade thickness was the governing factor in blade-twist considerations. For the same J range, propeller I twisted approximately nine times as much as propeller IV from which it differed only in thickness. Figure 9 has been prepared to show the difference in blade twist for propellers I and IV at 1600 rpm.

The other variable for the blades investigated was camber. Results of the investigation indicated that blade camber influences blade twist directly as it influences the section normal-force and pitching-moment coefficients. For the same J range, propellers II and III twisted about the same amount although the absolute values of twist were different. This is illustrated in figure 10 at 1600 rpm.

Effect of c_n and c_m on torsional deflection.- Figure 11 illustrates the effect of Mach number on blade loading and the resulting torsional deflection for propeller I operating at a J of 2.30. As the loading increases, blade twist also increases and when the loading drops off at the higher Mach numbers, blade twist will decrease and even go negative. The purpose of the figure is not to indicate any direct proportionality between blade loading and blade twist because it is realized that factors other than loading influence the blade twist. It is intended, however, to show that blade loading may have an appreciable bearing on blade twist but is not necessarily the principal factor governing blade twist as demonstrated by figure 12. In this figure, normal-force coefficient, pitching-moment coefficient, and blade twist have been plotted against fraction of tip radius for two propellers, differing only in design lift coefficient (propellers II and III) operating at a J of 2.00 at 1500 rpm. Despite the higher loading on propeller III, propeller II exhibits a higher value of measured blade twist. Upon an inspection of the moment-coefficient curves and the equation previously given for the aerodynamic twisting moment, it is readily seen that the difference in the pitching-moment coefficient explains the difference in the blade twist.

Relative contribution of M_a, M_p, and M_c to twist.- Two examples are illustrated in figure 13 to show the contribution of the elements comprising twist for two representative cases for propeller I. At 1140 rpm, $J = 2.00$ (fig. 13(a)) and at 1600 rpm, $J = 2.25$ (fig. 13(b)) the results indicate that the two centrifugal moments do not exactly cancel but contribute a net positive twist which is added to the aerodynamic twist, also positive in this case. Reference to equations (2) and (3) indicates that for a given blade geometry the summation of

centrifugal blade twist is a direct function of the square of the rotational speed, neglecting the second-order effects on blade angle caused either by blade loading or by blade rotation. Therefore, the contribution of the centrifugal moments will increase with rotational speed.

Comparison of measured and computed twist.- In general, the agreement between measured and calculated data is good. Most of the data agree within 0.1° to 0.2°. Occasionally discrepancies larger than 0.2° do occur and when they do it is usually for the highly loaded condition. This was especially prevalent for propeller III. No definite explanation of the variation between measured and calculated data can be offered. It is possible though since the discrepancies occur for runs near the force-break Mach number that a sensitive loading condition may prevail.

It has been shown that the propeller designer having sufficient aerodynamic data can calculate blade twist accurately within a few tenths of a degree. Figure 14 further indicates the good agreement between measured blade twist, calculated blade twist based on pressure-distribution data, and calculated blade twist based on two-dimensional data, for propeller III operating at 1140 rpm and a J of 1.80. The two-dimensional blade-section data used in the calculations were obtained from reference 9.

Twist and propeller characteristics - an example.- The efficiency of propeller I has been computed first as a rigid blade, not subject to twist, and secondly as a blade with an assumed radial twist distribution having a negative value of 2.0° at the tip. The operating conditions selected for the computations were $M = 0.60$ and $J = 2.25$. It was found that the imposed twist distribution decreased the efficiency slightly. The corresponding change in power coefficient, however, was about 23 percent.

A third computation was made in an effort to bring the power coefficient back to its original value which would correspond to the normal operation of an automatic pitch-change mechanism. It was therefore necessary to increase the blade angle about 1°. The blade-twist and blade-angle changes for the operating conditions imposed on the blade caused changes in the blade loading distribution (fig. 15). The final twisted blade approaches a Betz loading, but for the conditions imposed, the changes were so slight as to result in only small efficiency changes. For some conditions, notably take-off and excessively high section Mach numbers, small changes in blade angle may result in large changes in efficiency. The point of interest is that, although twist considerations may have little bearing on efficiency, the twist should be considered in a careful design of thin blades because the effect on power coefficient, and resulting operating blade angle, may be appreciable.

[redacted]

The correct angle of attack of a blade section must be determined in the propeller design stage, and therefore errors in the induced angle α_i (fig. 16) or in blade twist $\Delta\beta$ affect the accuracy of the design. The approximate methods of determining α_i are adequate for this design work, but the error which may be introduced by ignoring completely the blade twist $\Delta\beta$, as has usually been done, can be large.

Effect of plan form on blade twist.- Although thin propellers appear undesirable from the standpoint of blade twist, it should be pointed out that another trend, the use of wide blades in the design of high-speed propellers, can influence the amount of blade twist. The effect on blade twist for three blades differing only in plan form is shown in figure 17. For the comparison, propeller II was chosen as the basic blade operating at 1600 rpm and a $J = 2.20$. Blade II_A is a rectangular blade similar to propeller II except it has twice its chord. Blade II_B is also similar to blade II except it is a tapered blade having blade II_A's chord at the spinner and blade II's chord at the tip. The activity factors of the plan forms chosen are such that the total power absorbed would be approximately the same for four-, two-, and three-blade propellers, respectively. The same normal-force and pitching-moment coefficients obtained during the pressure-distribution investigation of blade II were used to calculate the twist for blades II_A and II_B. The wide blade, blade II_A, twists the least of the three blades because its section stiffness factors compared with blade II are in the ratio of the fourth power of the chord lengths. The aerodynamic twisting moment, however, is increased only in the ratio of the square of the chord lengths.

Concluding remarks.- The amount of twist a propeller blade experiences is the result of many factors. These factors can be classified into two groups. One group contains the geometric properties of the blade such as: thickness ratio, blade material, plan form, and pitch distribution. The second group is composed of factors arising from propeller operation which tend to produce a net twisting moment on the blade. Attempts to adjust the parameters in either group, to minimize the effect of blade twist, may not be feasible from a design standpoint although there are certain trends such as the use of wide blades that may be advantageous. The parameters affecting the efficient and safe operation of a high-speed propeller will always be of primary importance in the design. Therefore the designer may be able to cope with the problem of blade twist only by including some portion of the expected twist in the opposite sense at the design stage of a propeller.

[redacted]

CONCLUSIONS

Measurement and calculation of blade torsional deflection for the four blades investigated led to the following conclusions:

1. The magnitude of blade torsional deflection was not negligible and varied with blade design, the thinner the blade the greater the deflection. The thinnest blade deflected through a range of 4.9° at $x = 0.9$.

2. Blade torsional stiffness could be computed with good accuracy. The variation of section camber in the range of design lift coefficient, 0 to 0.5, for blades having equal distribution of section thickness ratio, had a negligible effect on this blade stiffness. Section camber affects blade torsion directly only as it affects the aerodynamic twisting moment.

3. Blade twist can be computed from a knowledge of section physical characteristics, the aerodynamic forces acting on the blade, and propeller operating conditions. The comparison of computed and measured torsional deflections indicated good agreement.

4. Blade torsion can have an appreciable effect on the radial distribution of aerodynamic load which in turn affects operating blade angle and propeller efficiency. Blade twist should therefore be considered in the design of thin propeller blades.

Langley Aeronautical Laboratory
National Advisory Committee for Aeronautics
Langley Field, Va.

[redacted]

APPENDIX

DESCRIPTION, CALIBRATION, AND OPERATING PROCEDURE OF OPTICAL DEFLECTOMETER

General description.- The optical deflectometer was made by adapting an airplane sighting station for use as a modified theodolite in this investigation. A cone of light was transmitted along the optical axis and a portion of this light was reflected from a small mirror attached to the propeller blade. The reflection could be seen only when the mirror surface was normal to the optical axis. The sighting station is the main component of the optical deflectometer and reduced to essentials is nothing more than two periscopes placed end to end with a common eyepiece and a hinged mirror to enable selection of the periscope desired. The lower periscope only was used for the present instrument. A complete description of the sighting station is given in reference 10.

A photograph of the assembled optical deflectometer is shown in figure 18, and a diagram showing the lower dome of the deflectometer and dynamometer in their approximate locations with respect to the Langley 16-foot high-speed-tunnel test section is shown in figure 19. The sighting station was supported by two lathe crossheads, one to give a fine adjustment of fore-aft position, and the other to give a fine adjustment sidewise. The crossheads were in turn secured to a carriage which rolled along tracks on the top of the tunnel, thus providing a coarse position adjustment. Prior to each group of measurements the carriage was firmly secured to the tunnel tracks, thus limiting the amount of forward and rearward sight travel to the maximum travel of the crosshead, and the angle of the sight λ was also set.

The hand grips located at approximately the middle of the main tube control the azimuth and elevation of the line of sight through motion of the lower prism. Rotation of the hand grips about an axis normal to the axis of the main tube actuated the lower prism by means of a drive shaft and gear mechanism and the direction of the line of sight in elevation was measured by a selsyn generator.

The lower dome is essentially a protective covering for the lower prism and drive gears. As shown in figure 19, an external light source and fairing were attached to the lower dome. Light from a concentrated arc light was collected by a lens system (f = 4.5, 76 mm) and directed to a partially silvered mirror in the lower dome. The light rays were then reflected from this mirror to the adjustable prism and out of the sight as a cone of light which became approximately 4 inches in diameter at the propeller blade. When the light rays impinged normal to the

[redacted]

blade mirror, some returned along the same light path and were viewed as a short streak of light by the observer. The adjustable prism had to be tilted by an amount which was a direct measure of the angle of blade torsional deflection at that station.

Geometry of optical path.- The deflection could be measured at only one blade station at a time and the angle of sight inclination was chosen for each station so that a plane through the axis of the sight parallel to the tunnel axis would be tangent to the circle described by the station at which measurements were being made. As shown in figure 20(a), assuming no bending deflection, only one plane is swept out by the beam of light perpendicular to the blade mirror (ABB'). This plane intersects the tunnel wall in a straight line parallel to the tunnel axis; therefore, only axial movement of the sight is required to intercept the light beam regardless of blade-angle change within a conventional operating range. The axial view of this plane is therefore a single line which establishes the sight angle λ as a constant (fig. 20(b)). By this means the mathematics of determining blade deflections was reduced to its simplest form. Blade bending altered the plane of tangency slightly but not enough to change the station radius appreciably and consequently affect the accuracy of the instrument.

Calibration and accuracy of measurements.- Static calibration of the deflectometer was accomplished by sighting on a mirror attached to the movable section of a propeller protractor as the protractor reference face was moved along a straight edge. When the observer viewed the reflected light, a reading of the protractor and elevation selsyn indicators was taken. A disc graduated in 1° increments was used to measure the position of the elevation selsyn arm. It was found that for a 1° change in mirror angle the indicator arm connected to the selsyn rotated through 31°. Therefore, a 1° change on the selsyn scale was equivalent to a 0.03° change in the line of sight, which agreed with the value given in reference 10. A number of readings were taken at each protractor setting and the results showed that the instrument could repeat a reading within $\pm 0.03^\circ$. Further static tests conducted with a mirror attached to a disc rotating at high speeds indicated that the same accuracy in repeating a reading existed.

When the deflectometer was mounted on the tunnel tracks, the lower dome protruded about 4 inches into the tunnel. An investigation was therefore conducted to determine the amount of deflection of the instrument under operating conditions. A mirror was attached rigidly to the tunnel wall some distance upstream of the deflectometer and a number of observations were made at tunnel speeds varying from zero to maximum velocity. The correction determined therefrom has been applied to all data presented herein. For speeds up to 180 miles per hour the correction was zero, and from 180 to 460 miles per hour the correction varied linearly from 0 to 0.14°. No investigation was conducted to determine

[redacted]

if the dynamometer deflected because the negligible twist measured on propeller IV, the thick propeller, at the $x = 0.45$ station, indicated no operational dynamometer deflections.

It is believed that the optical deflectometer measured blade twist within 0.10°, as indicated by the repeatability of the data.

Operating procedure.- Prior to starting a run, the sight angle was set for the particular station to be investigated and the carriage was firmly secured to the tunnel tracks downstream of the propeller. The instrument was zeroed before each run by obtaining an initial reading on the selsyn indicators of the prism position required to view the light reflected from the stationary blade. The location downstream of the propeller depended upon the blade-angle setting for the station under consideration. Inboard sections, with their high blade angles, required that the deflectometer be located relatively close to the propeller. The outboard station with its low blade angle required that the deflectometer be located farther from the propeller even though this geometric twist was partly compensated for by tilting the mirror on the blade.

The reflected light as viewed by the observer appeared as a short narrow streak. When the light streak was alined with the dot in the center of the sighting-station reticle the camera shutter release was tripped. As the load on the propeller was increased, the blade twist changed in the direction of increasing blade angle and the sighting station was moved upstream until the observer once again could view the reflected light. During a run the operator scanned a portion of the tunnel wall that corresponded to the same portion he saw after the zero reading had been taken with the propeller rotated out of the field of view. This scanning operation facilitated locating the mirror image because it defined the proper field of view.

As the operators became familiar with the operation of the sighting station it was possible to investigate propeller blade twist and pressure distribution simultaneously although some time penalty was imposed which required limiting the number of blade-deflection measurement stations. The blade-twist indicator was installed beside the pressure-distribution tubes on the manometer board. A signal-system arrangement enabled the deflectometer operator to operate a camera at each test point thus obtaining a simultaneous reading of pressure-distribution and blade-twist data.

The data obtained from the pressure-distribution investigation were used to calculate the aerodynamic torsional moment. Knowing this moment, it was possible to calculate blade twist and compare this value with the measured values of blade twist. In general, the agreement between calculated and measured values of blade torsional deflection was good.

[redacted]

REFERENCES

1. Hartman, Edwin P., and Biermann, David: The Torsional and Bending Deflection of Full-Scale Aluminum-Alloy Propeller Blades under Normal Operating Conditions. NACA Rep 644, 1938.

2. Corson, Blake W., Jr., and Maynard, Julian D.: The NACA 2000-Horsepower Propeller Dynamometer and Tests at High Speed of an NACA 10-(3)(08)-03 Two-Blade Propeller. NACA RM L7L29, 1948.

3. Gray, W. H., and Hunt, Robert M.: Pressure Distributions on the Blade Sections of the NACA 10-(3)(049)-033 Propeller under Operating Conditions. NACA RM L9L23, 1950.

4. Johnson, Peter J.: Pressure Distributions on the Blade Sections of the NACA 10-(3)(090)-03 Propeller under Operating Conditions. NACA RM L50A26, 1950.

5. Evans, Albert J., and Luchuk, Wallace: Pressure Distributions on the Blade Sections of the NACA 10-(5)(066)-03 Propeller under Operating Conditions. NACA RM L50B21, 1950.

6. Steinberg, Seymour, and Milling, Robert W.: Pressure Distributions on the Blade Sections of the NACA 10-(0)(066)-03 Propeller under Operating Conditions. NACA RM L50C03, 1950.

7. Sterne, L. H. G.: The Structural Aspects of Propeller Design. Rep. No. Structures 5, British R.A.E., July 1947.

8. Wood, R. McKinnon, and Perring, W. G. A.: Stresses and Strains in Airscrews with Particular Reference to Twist. R. & M. No. 1274, British A.R.C., 1929

9. Lindsey, W. F., Stevenson, D. B., and Daley, Bernard N.: Aerodynamic Characteristics of 24 NACA 16-Series Airfoils at Mach Numbers between 0.3 and 0.8. NACA TN 1546, 1948.

10. Anon: Overhaul Instructions for Remote Control Turret System. Model 2CFR21B3 for A-26 Airplanes. AAF Publication AN 11-70A-13, March 15, 1945, pp. 136-176.

[redacted]

TABLE I

BLADE-ANGLE VALUES, β, DEGREES

x	Propeller I	Propeller II	Propeller III	Propeller IV
0.20	76.1	76.1	76.1	76.1
.25	72.5	72.3	72.3	72.3
.30	69.0	68.9	68.8	68.8
.35	65.6	65.6	65.5	65.5
.40	62.4	62.6	62.3	62.3
.45	59.3	59.5	59.3	59.3
.50	56.5	56.7	56.5	56.5
.55	53.8	53.9	53.8	53.8
.60	51.4	51.6	51.3	51.4
.65	49.1	49.4	49.2	49.1
.70	47.0	47.4	47.0	47.0
.75	45.0	45.2	45.0	45.0
.80	43.2	43.5	43.1	43.1
.85	41.5	41.9	41.1	41.3
.90	39.7	40.0	39.5	39.6
.95	38.1	38.9	38.4	38.3
.975	37.3	38.5	37.9	37.7

[redacted]

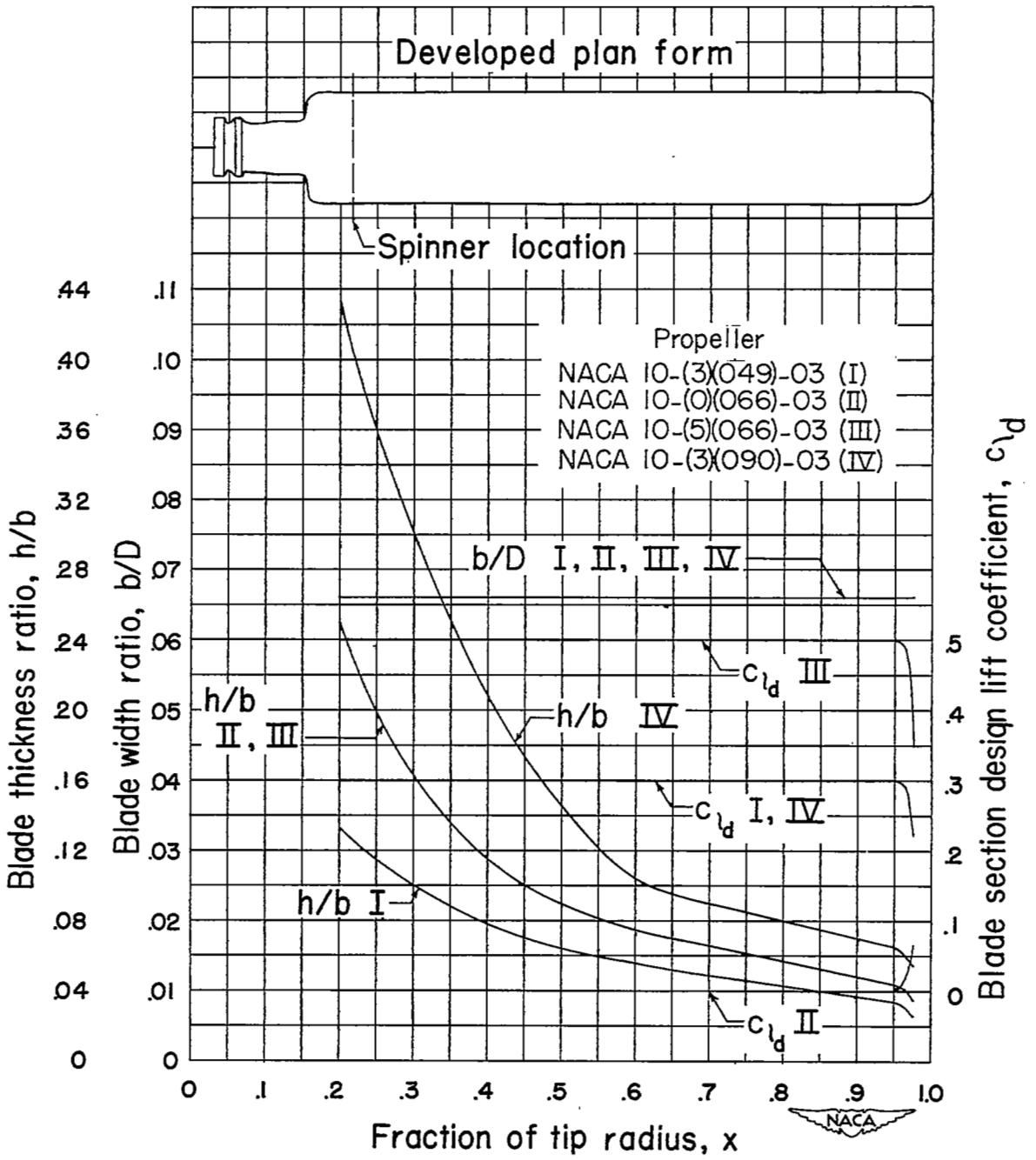

Figure 1.- Blade-form curves.

[redacted]

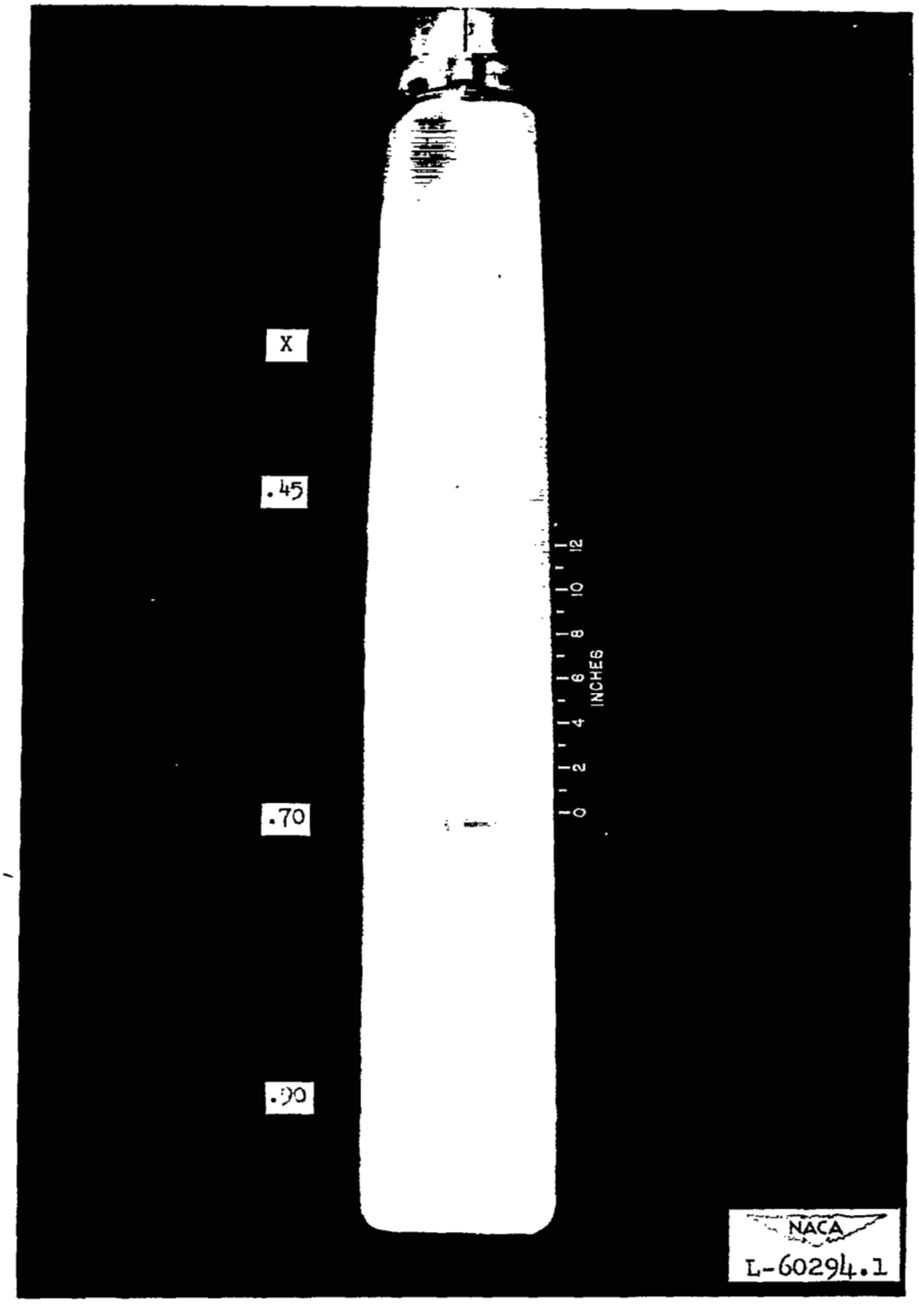

Figure 2.- Photograph of blade with attached mirrors.

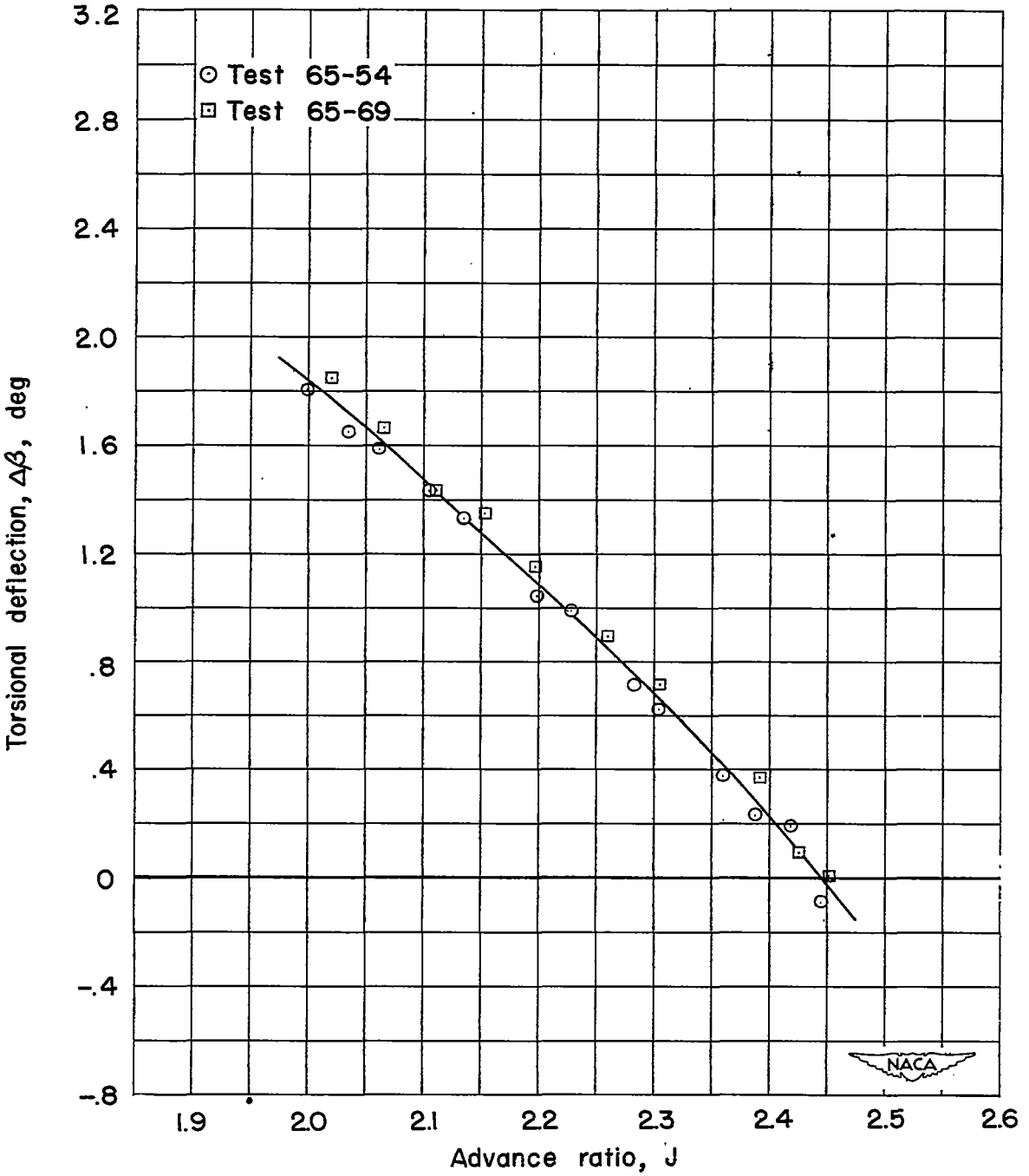

Figure 3.- Typical deflection data for NACA 10-(0)(066)-03 propeller (II) at 1600 rpm. $x = 0.90$; $\beta_{0.75R} = 45.2^{\circ}$.

[redacted]

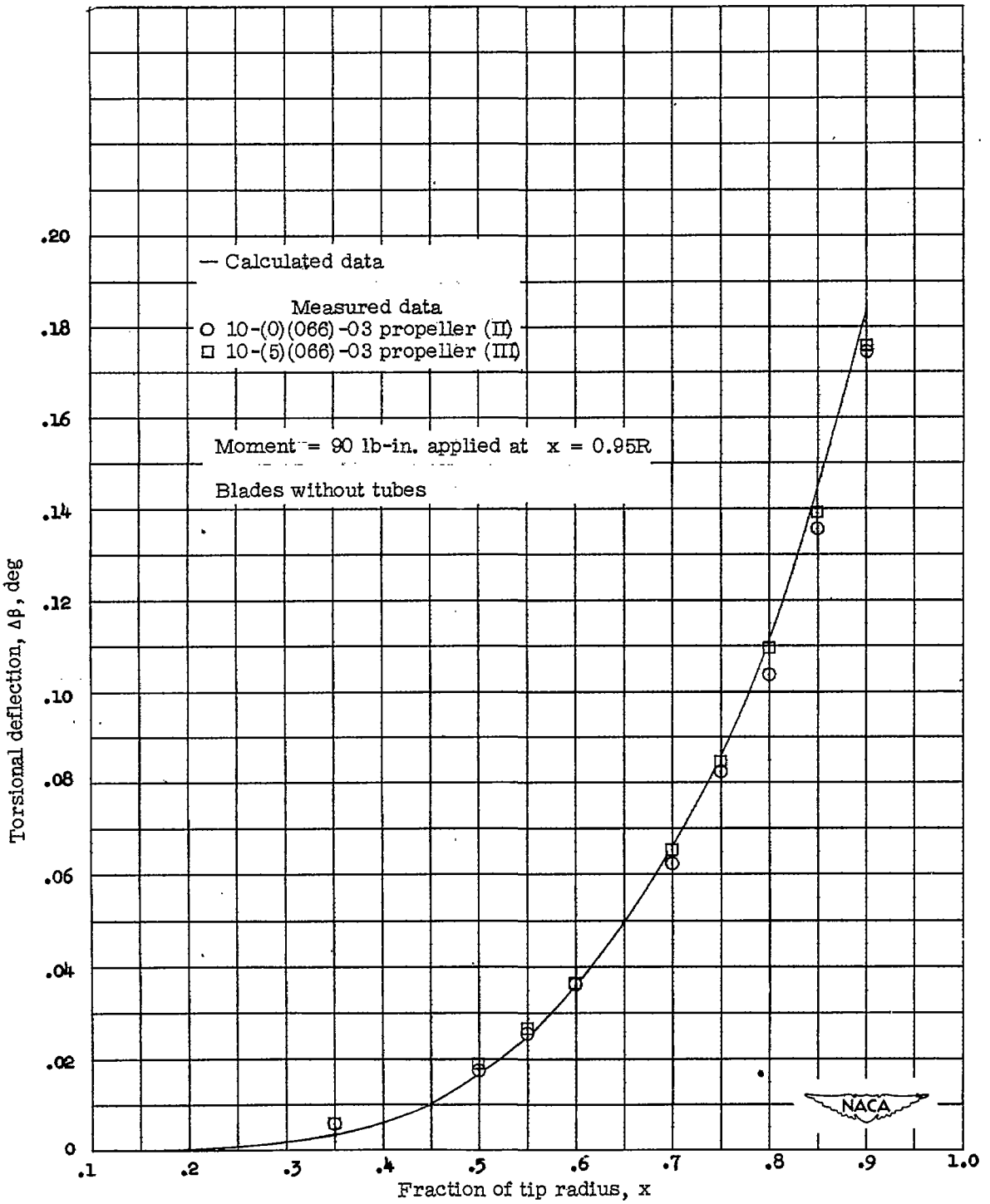

Figure 4.- Values of blade twist for a given applied moment for blades differing only in section camber.

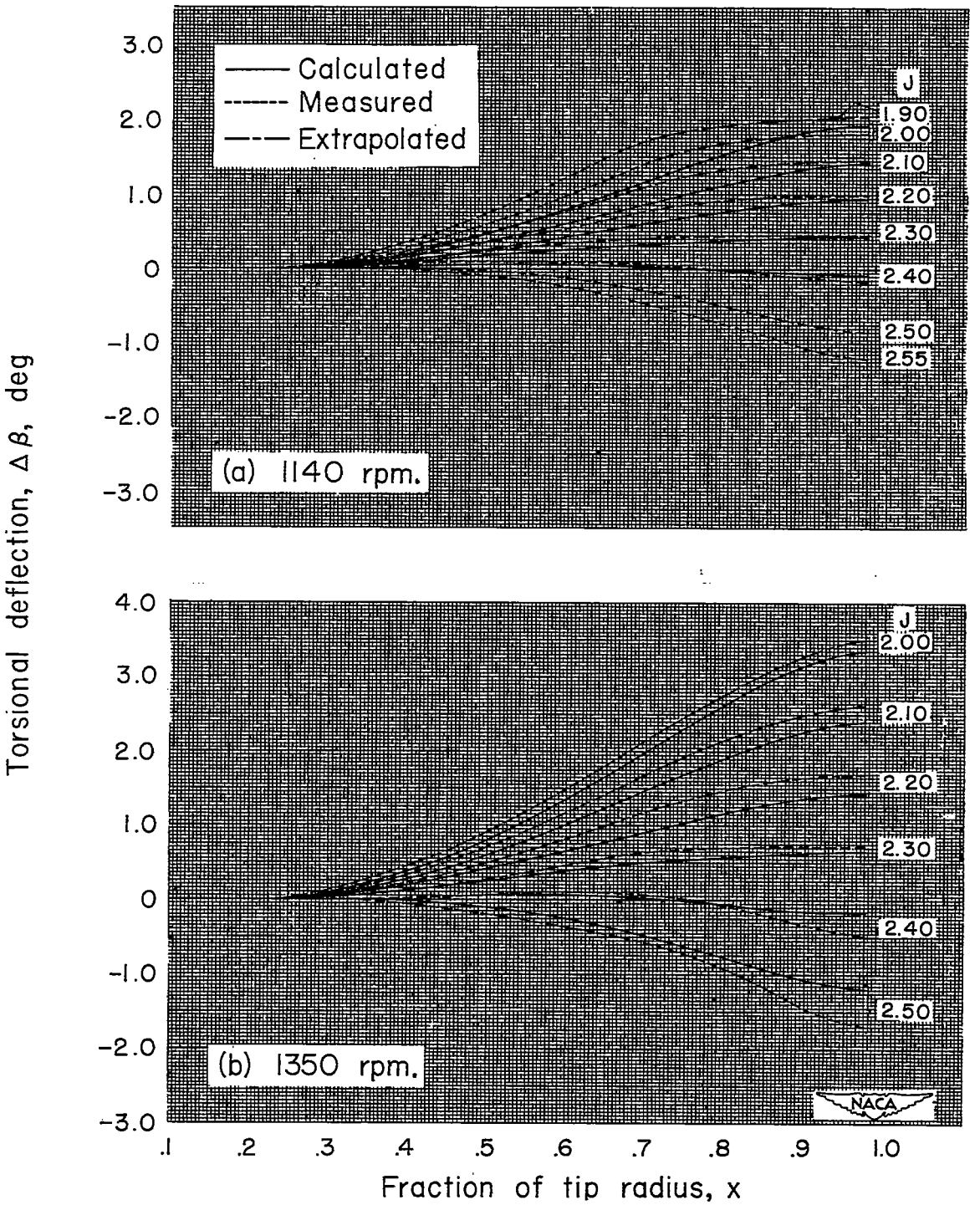

Figure 5.- Torsional-deflection curves for NACA 10-(3)(049)-03 propeller (I); $\beta_{0.75R} = 45.0°$.

[redacted]

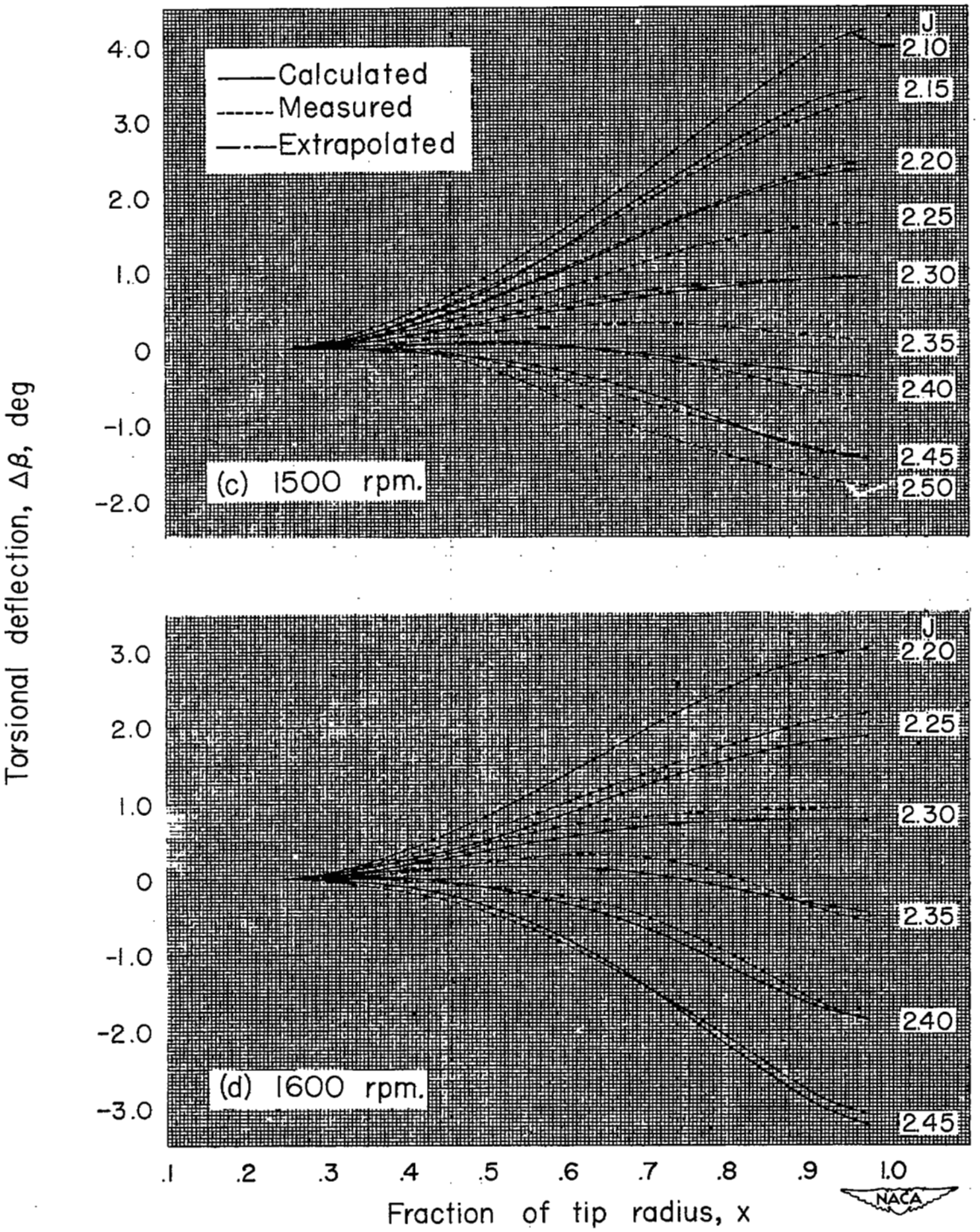

Figure 5.- Continued.

[redacted]

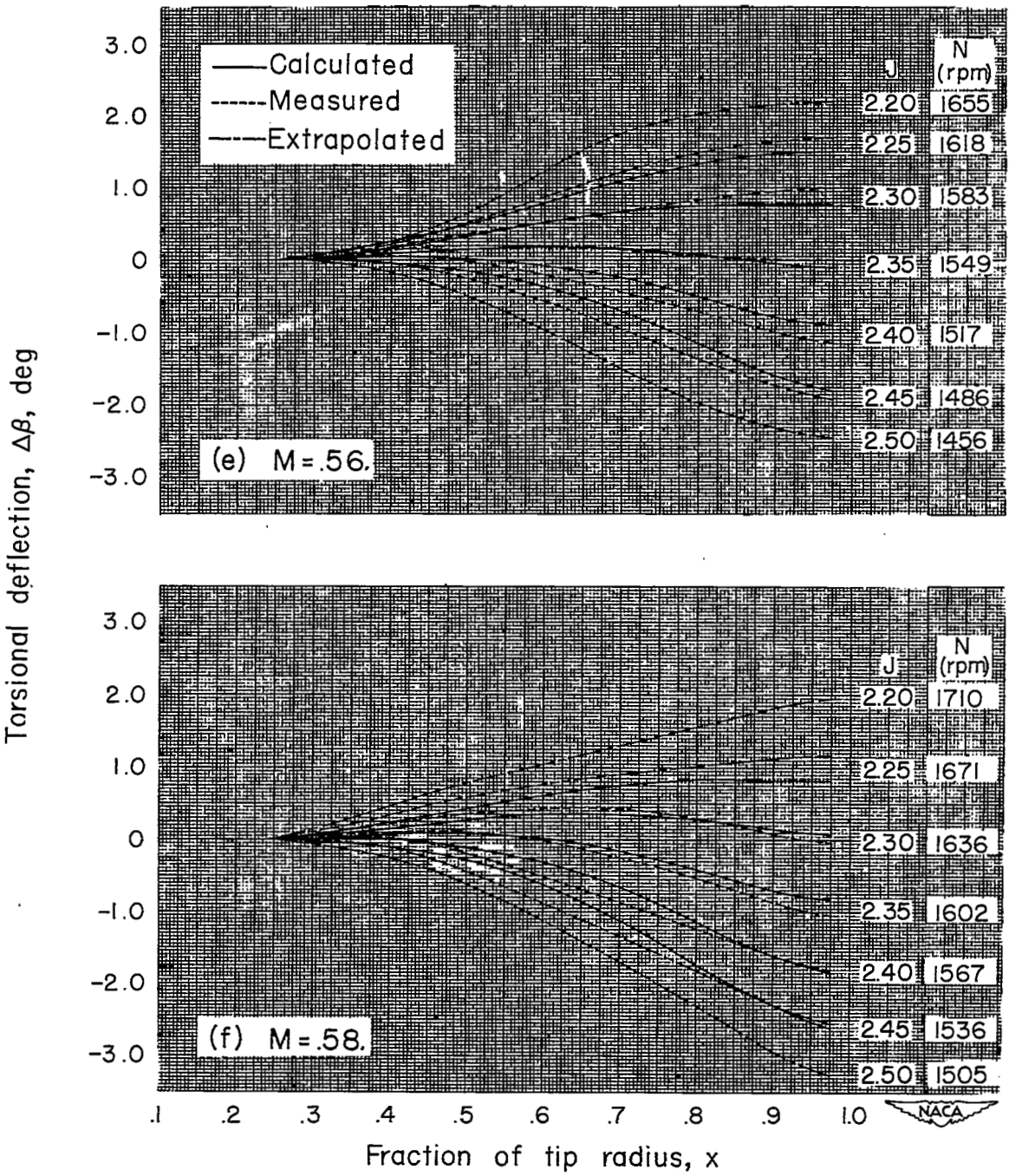

Figure 5.- Continued.

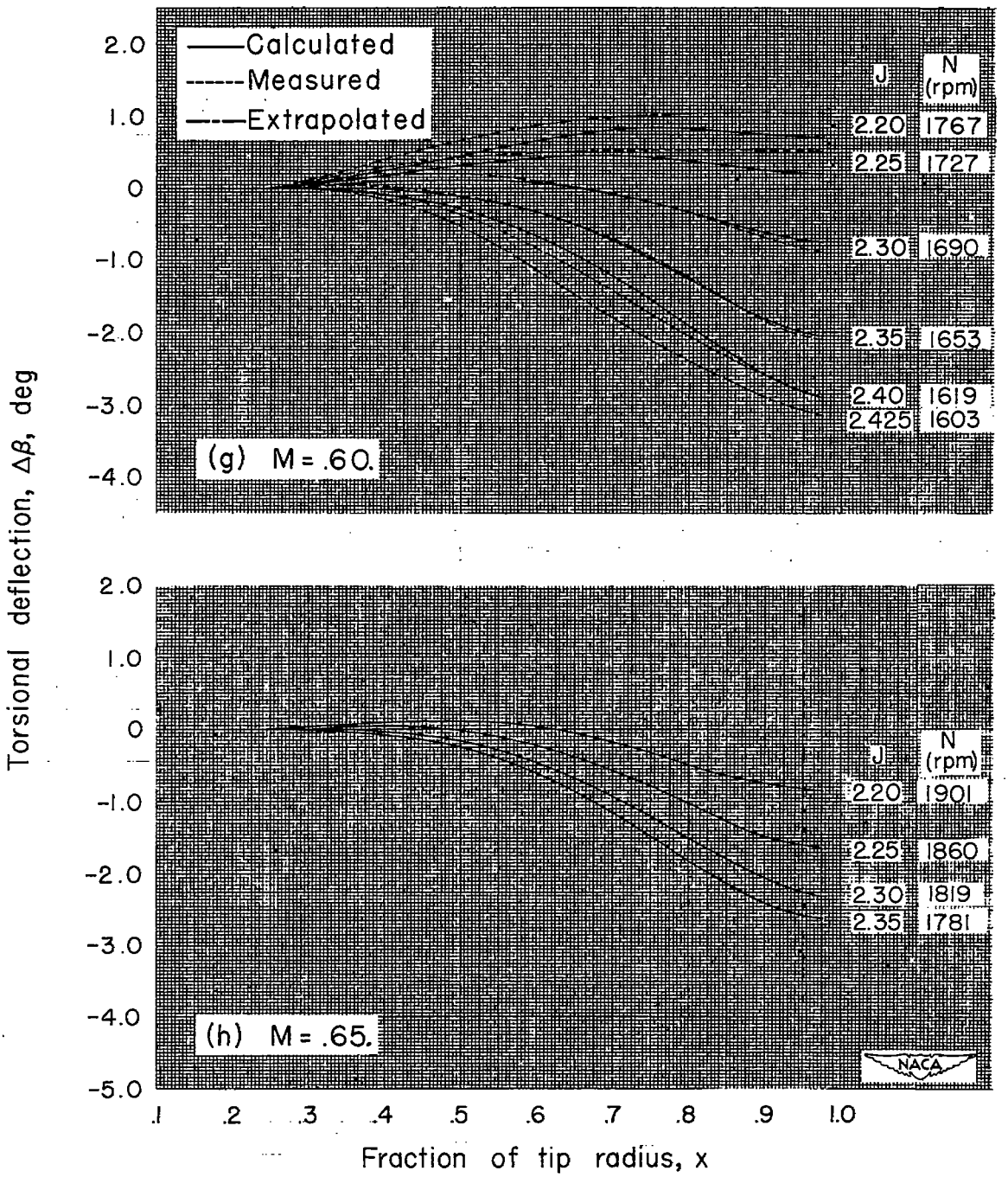

Figure 5.- Concluded.

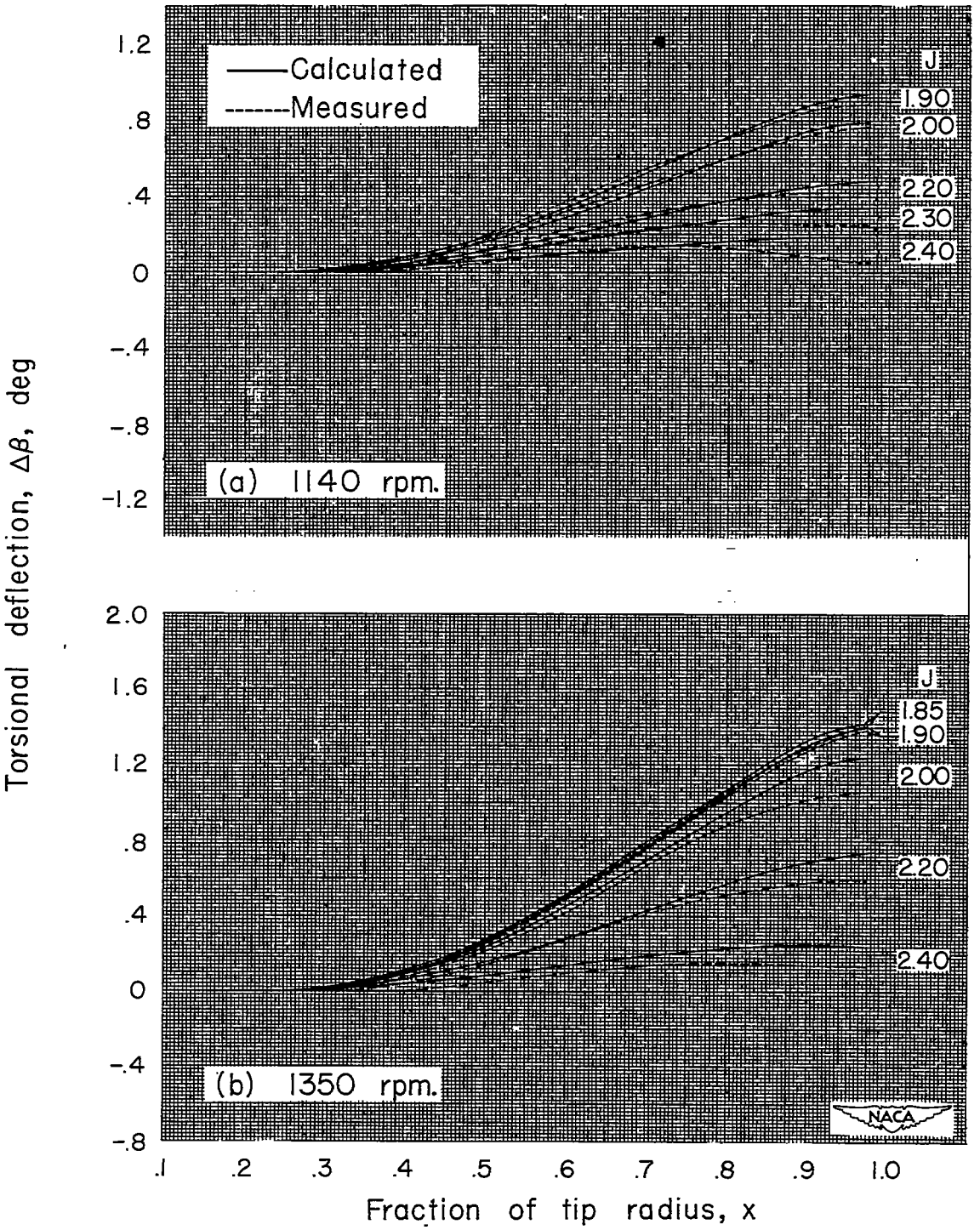

Figure 6.- Torsional-deflection curves for NACA 10-(0)(066)-03 propeller (II); $\beta_{0.75R} = 45.2^{\circ}$

[redacted]

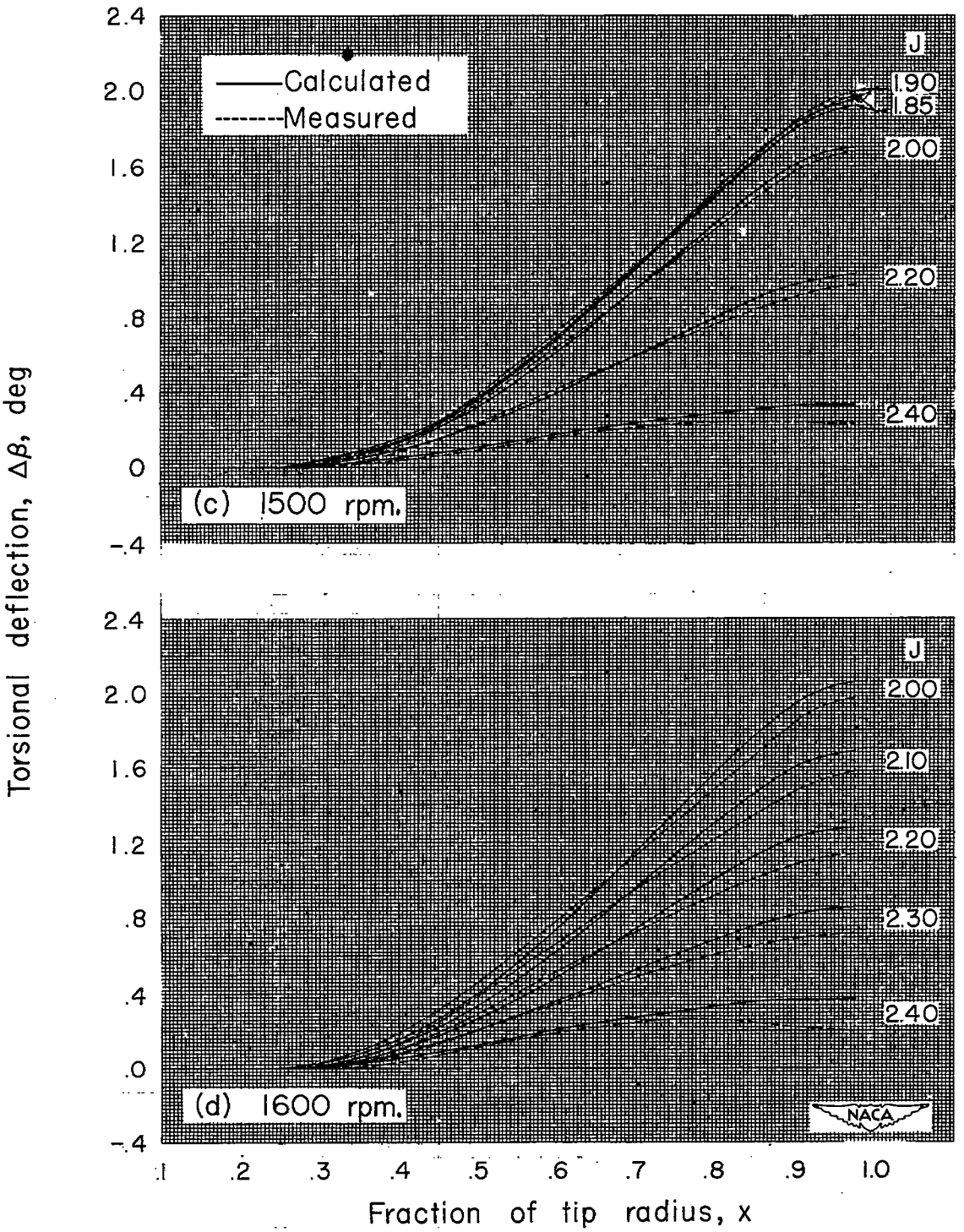

Figure 6.- Continued.

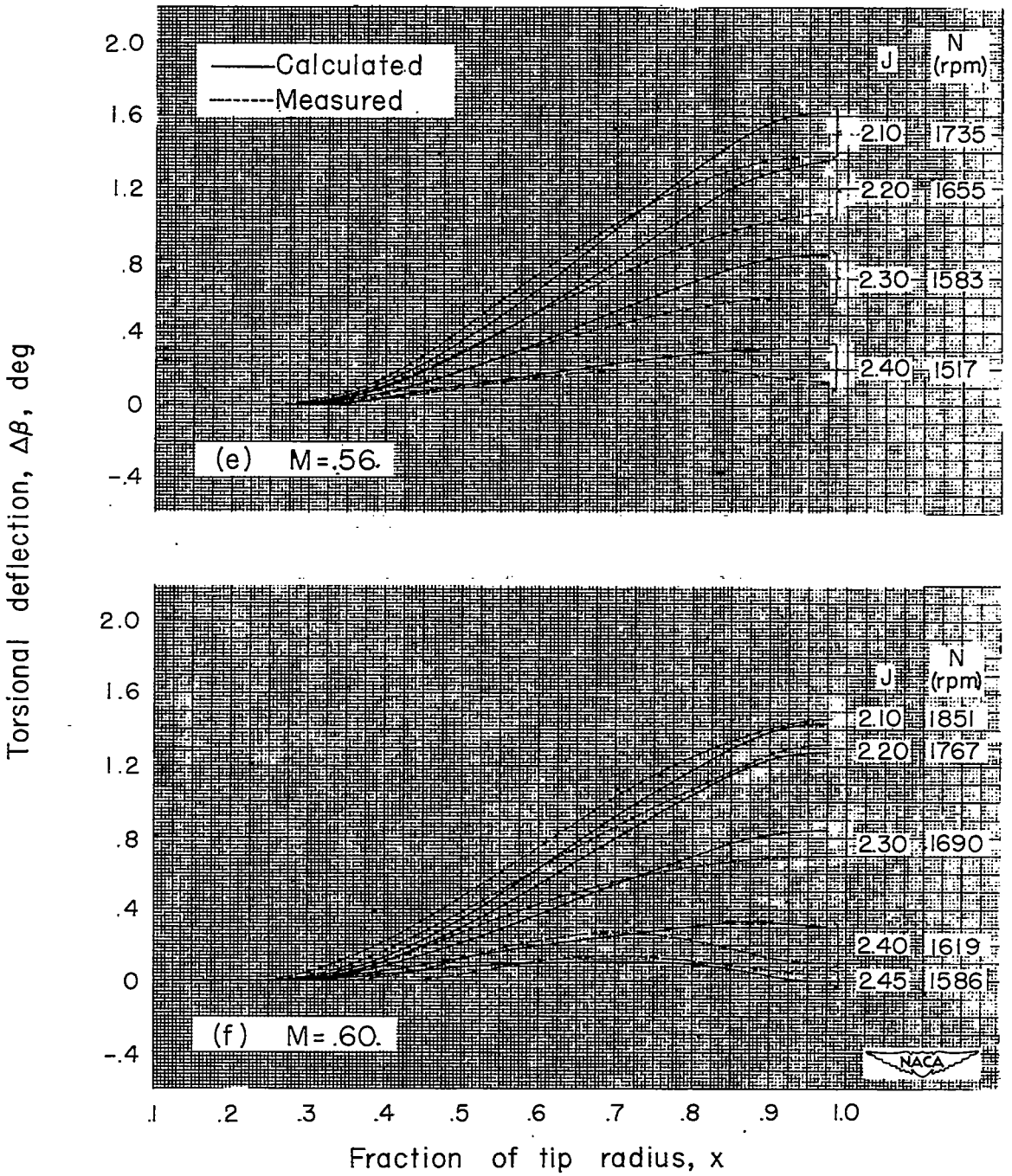

Figure 6.- Continued.

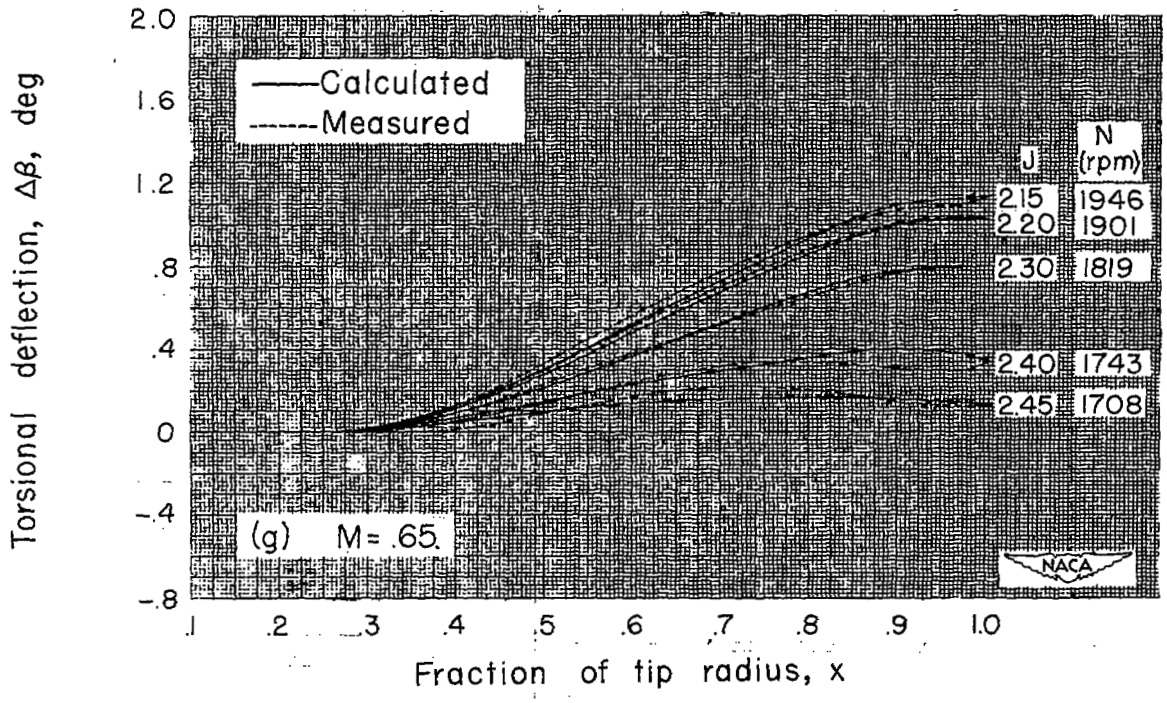

Figure 6.- Concluded.

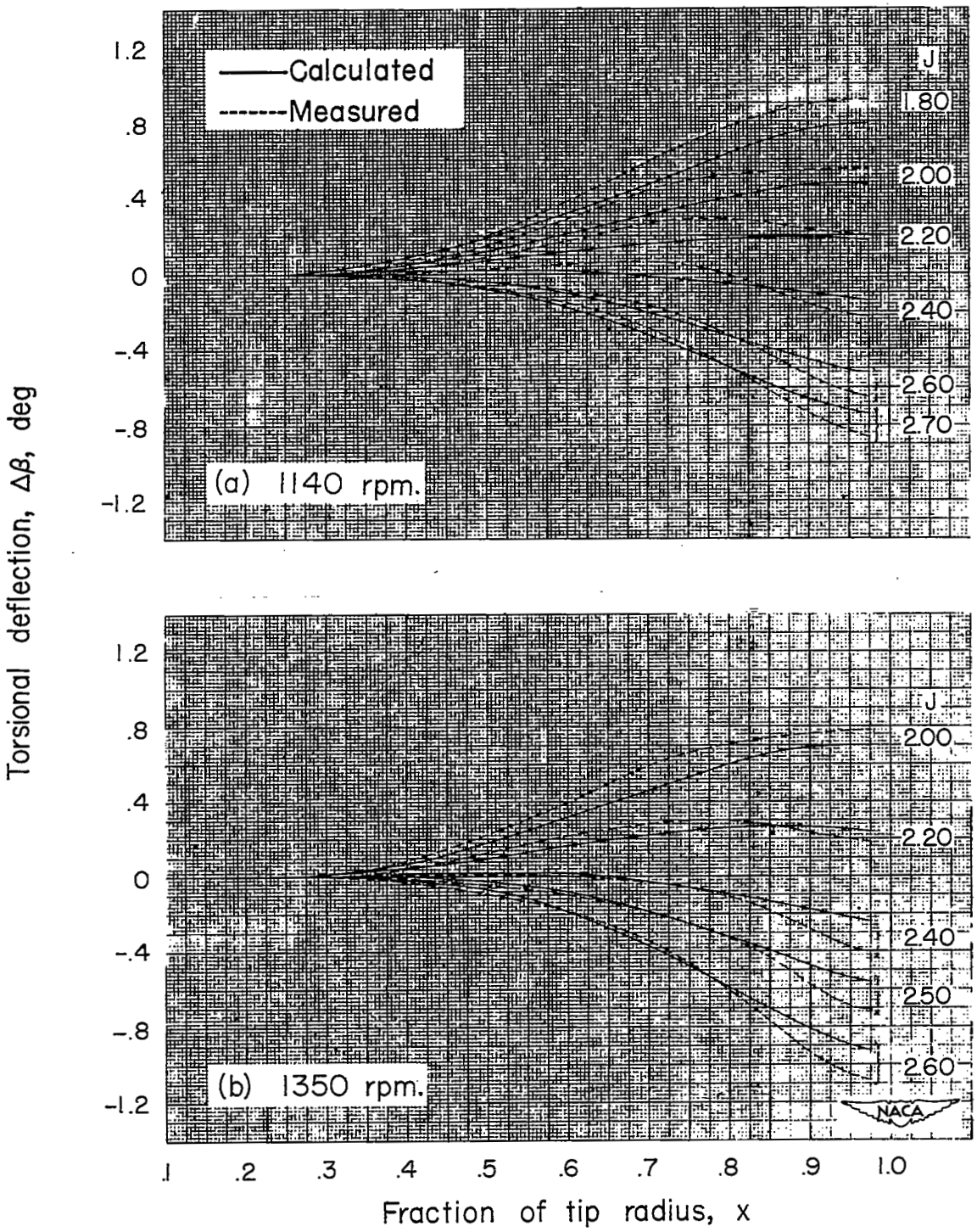

Figure 7.- Torsional-deflection curves for NACA 10-(5)(066)-03 propeller (III); $\beta_{0.75R} = 45.0°$.

[redacted]

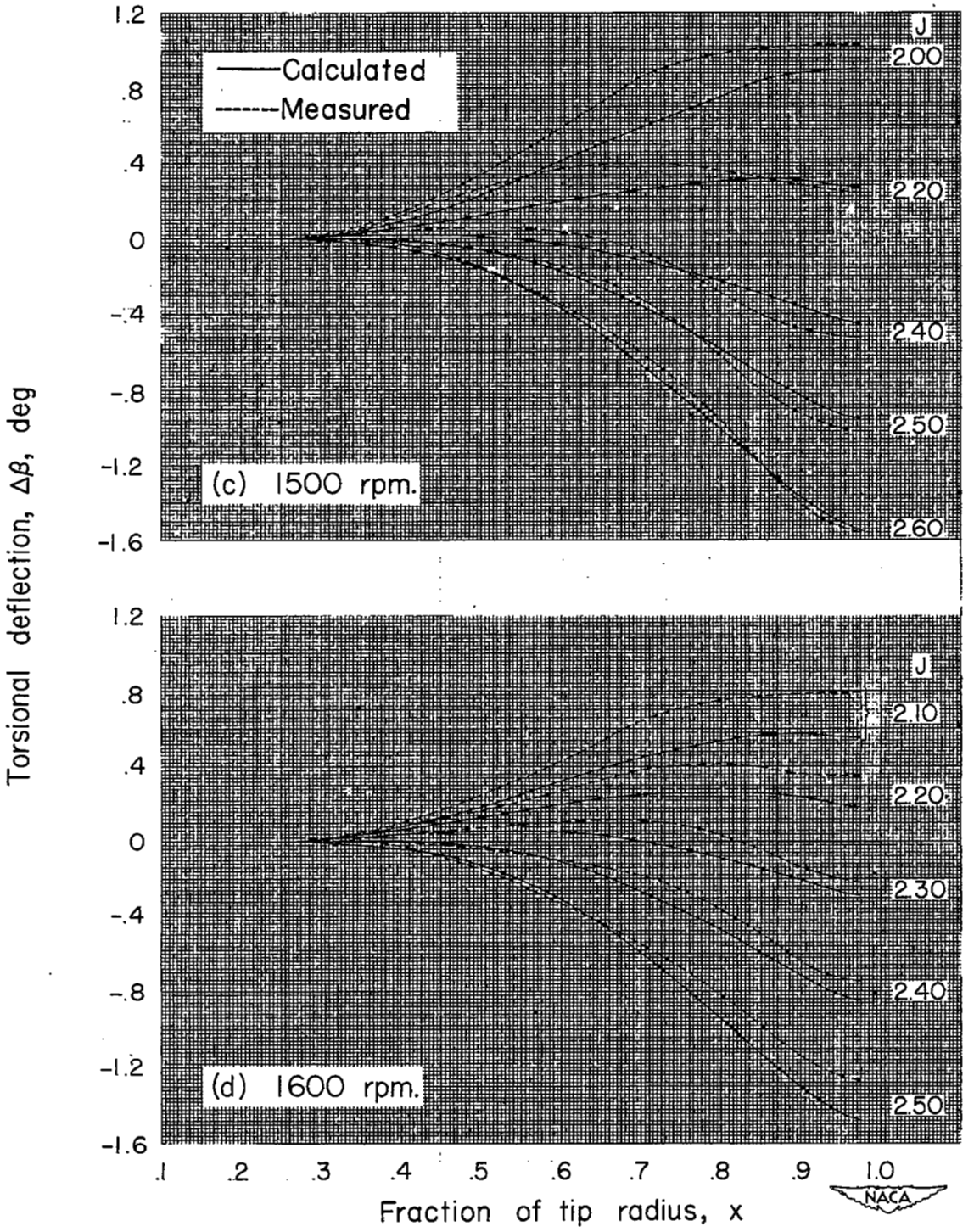

Figure 7.- Continued.

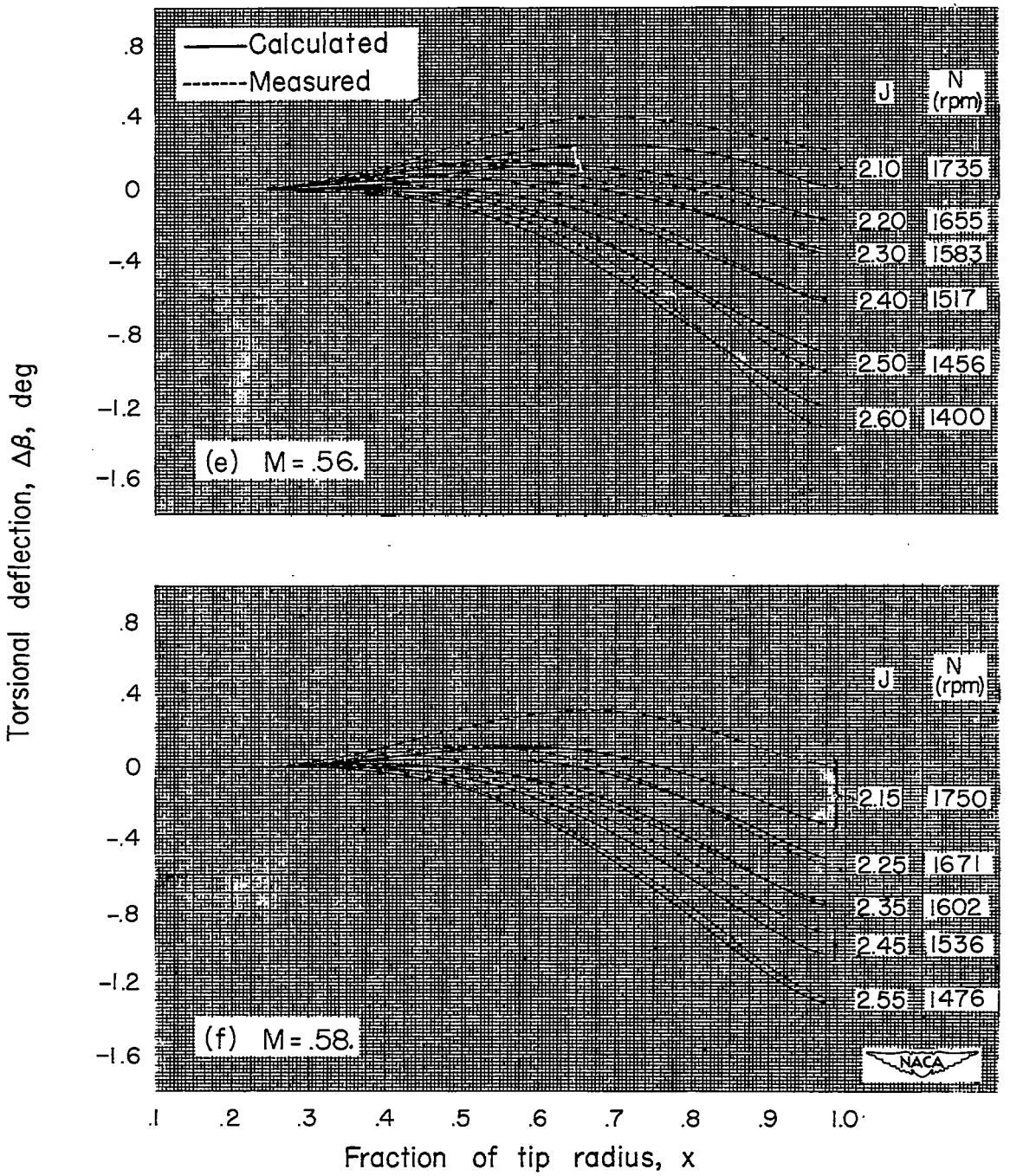

Figure 7.- Continued.

[redacted]

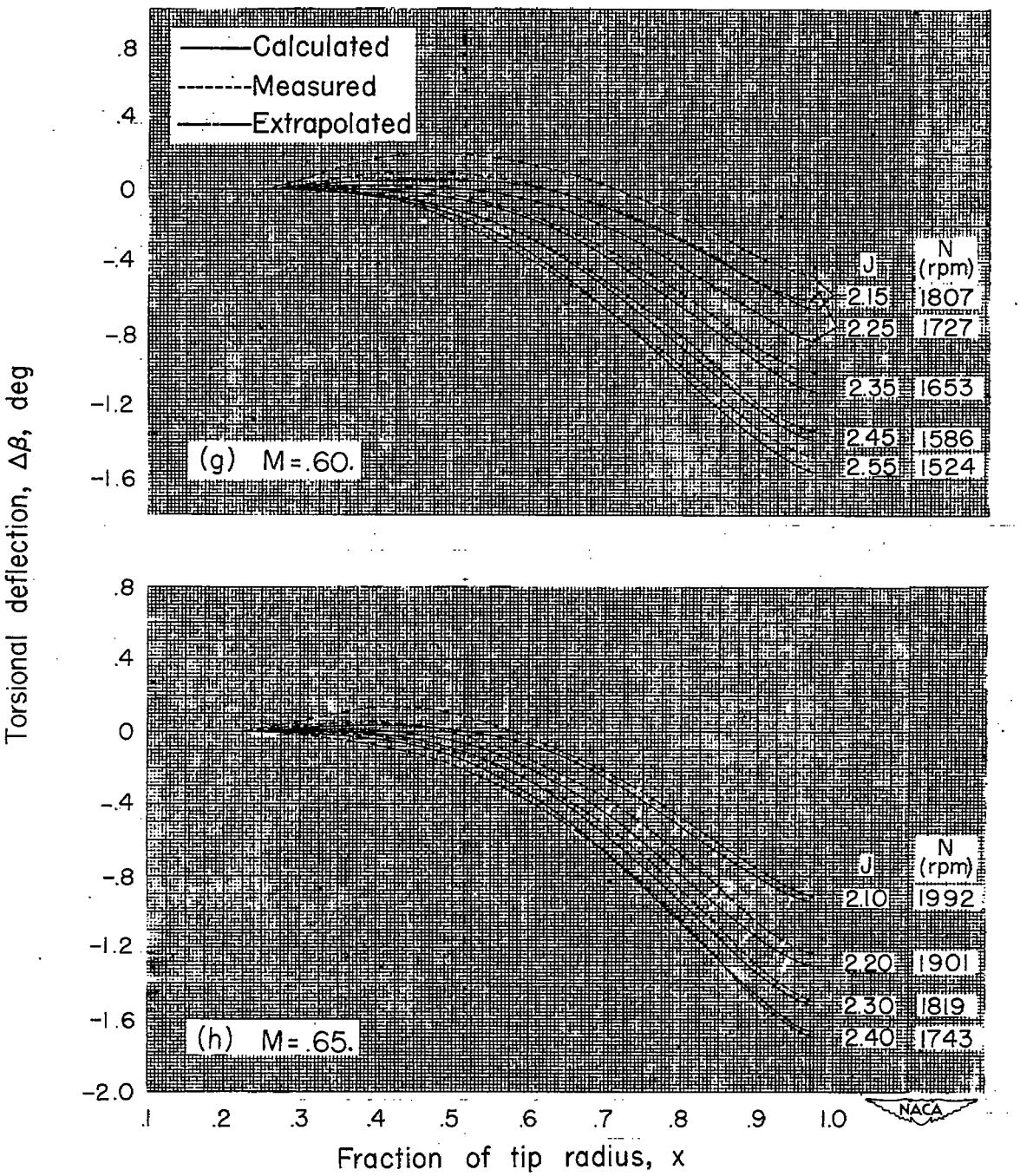

Figure 7.- Concluded.

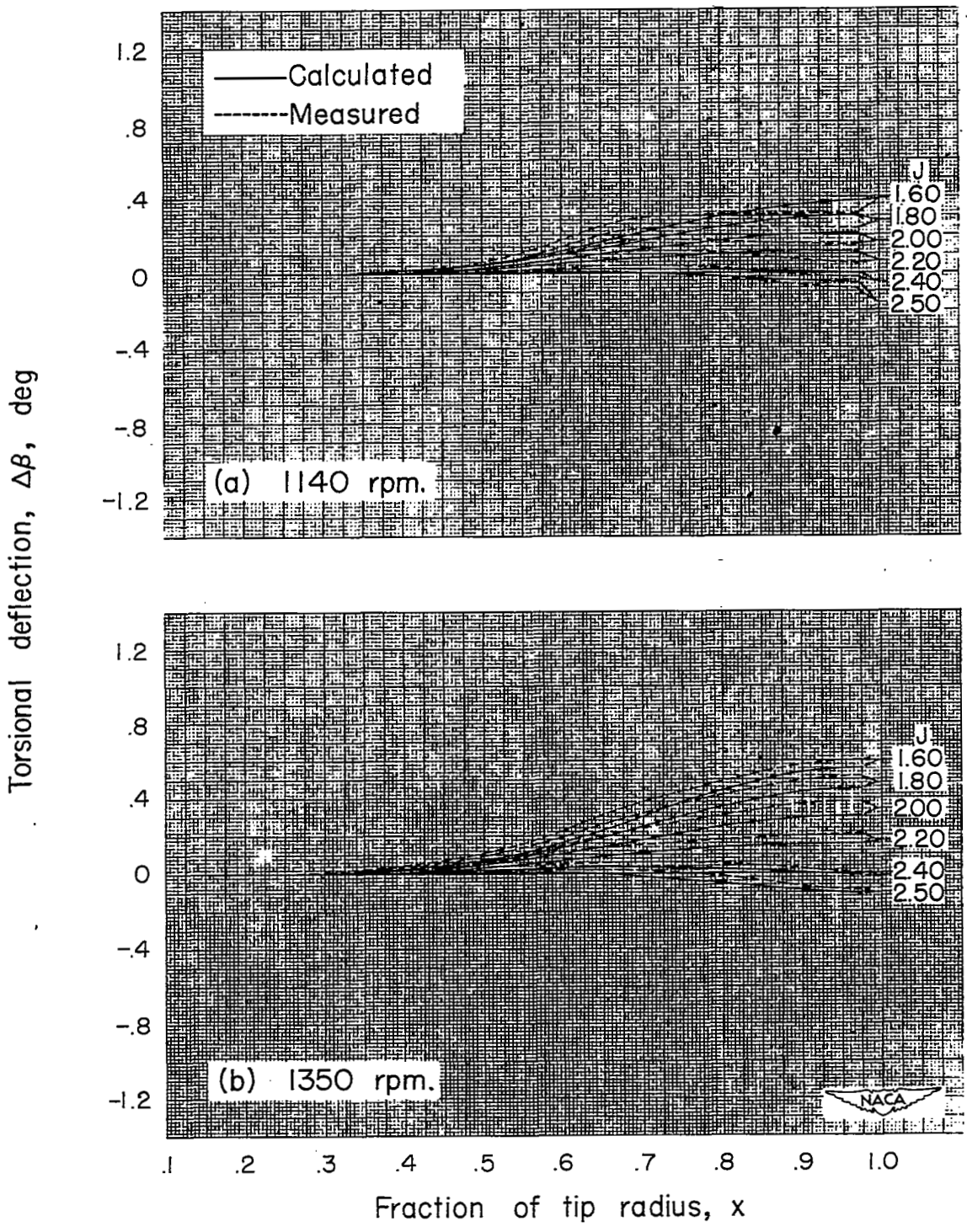

Figure 8.- Torsional-deflection curves for NACA 10-(3)(090)-03 propeller (IV); $\beta_{0.75R} = 45.0^{\circ}$.

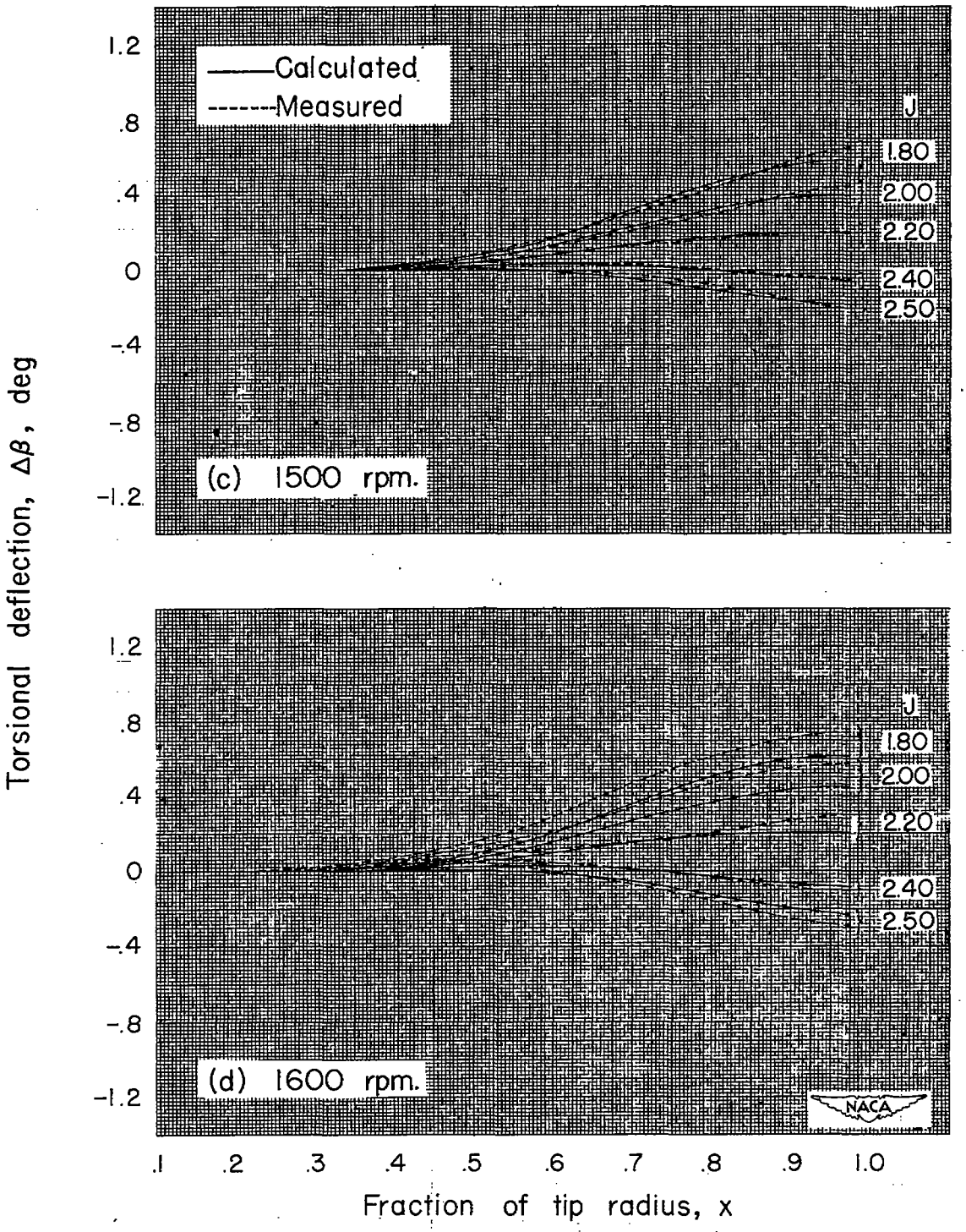

Figure 8.- Continued.

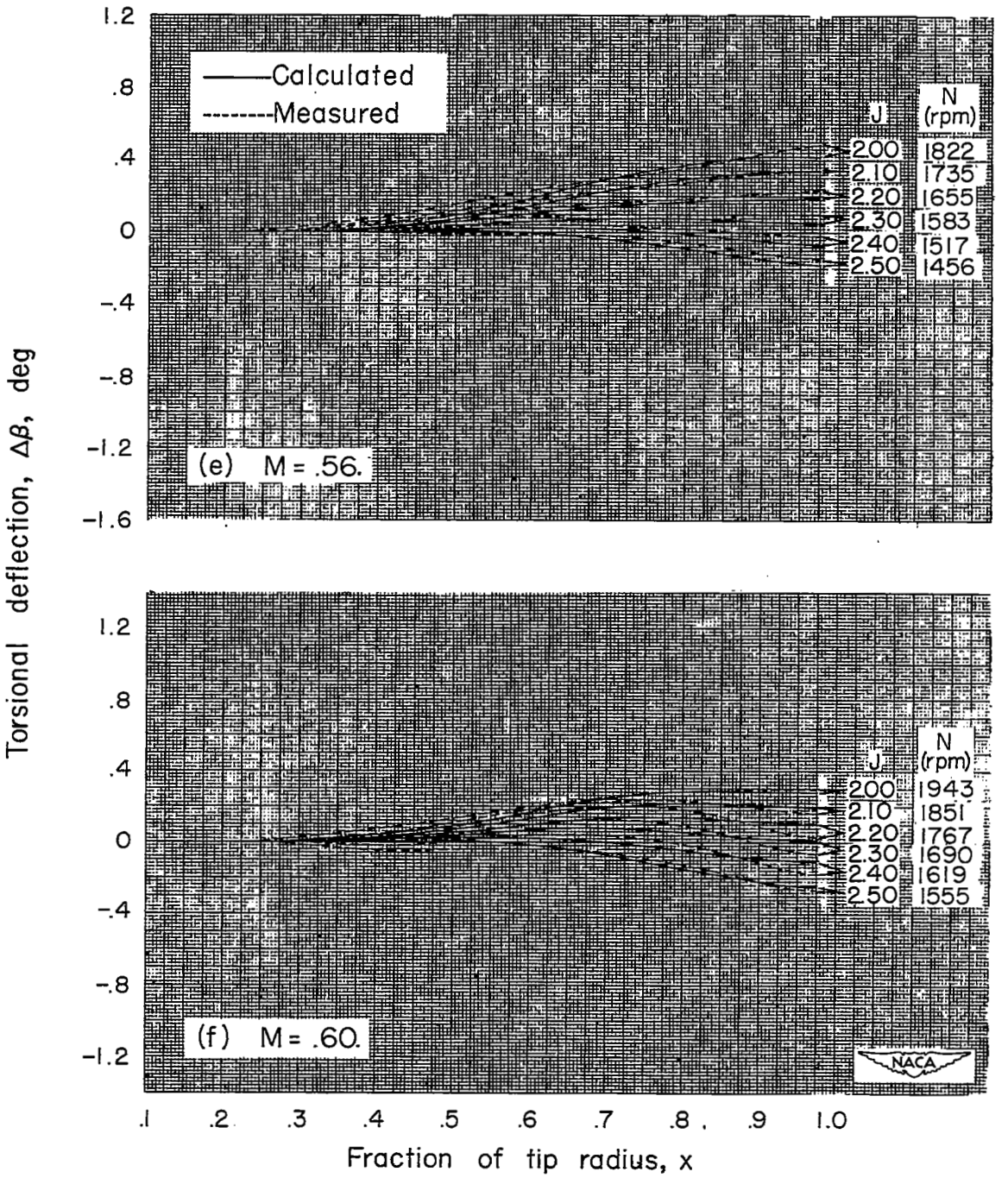

Figure 8.- Continued.

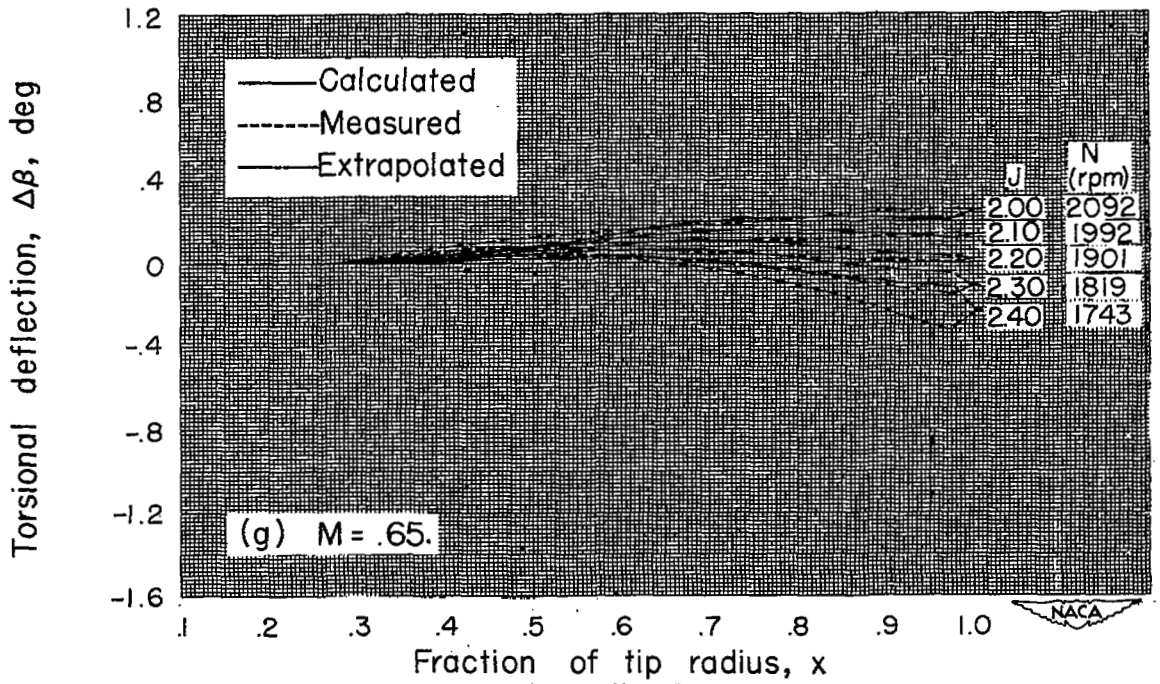

Figure 8.- Concluded.

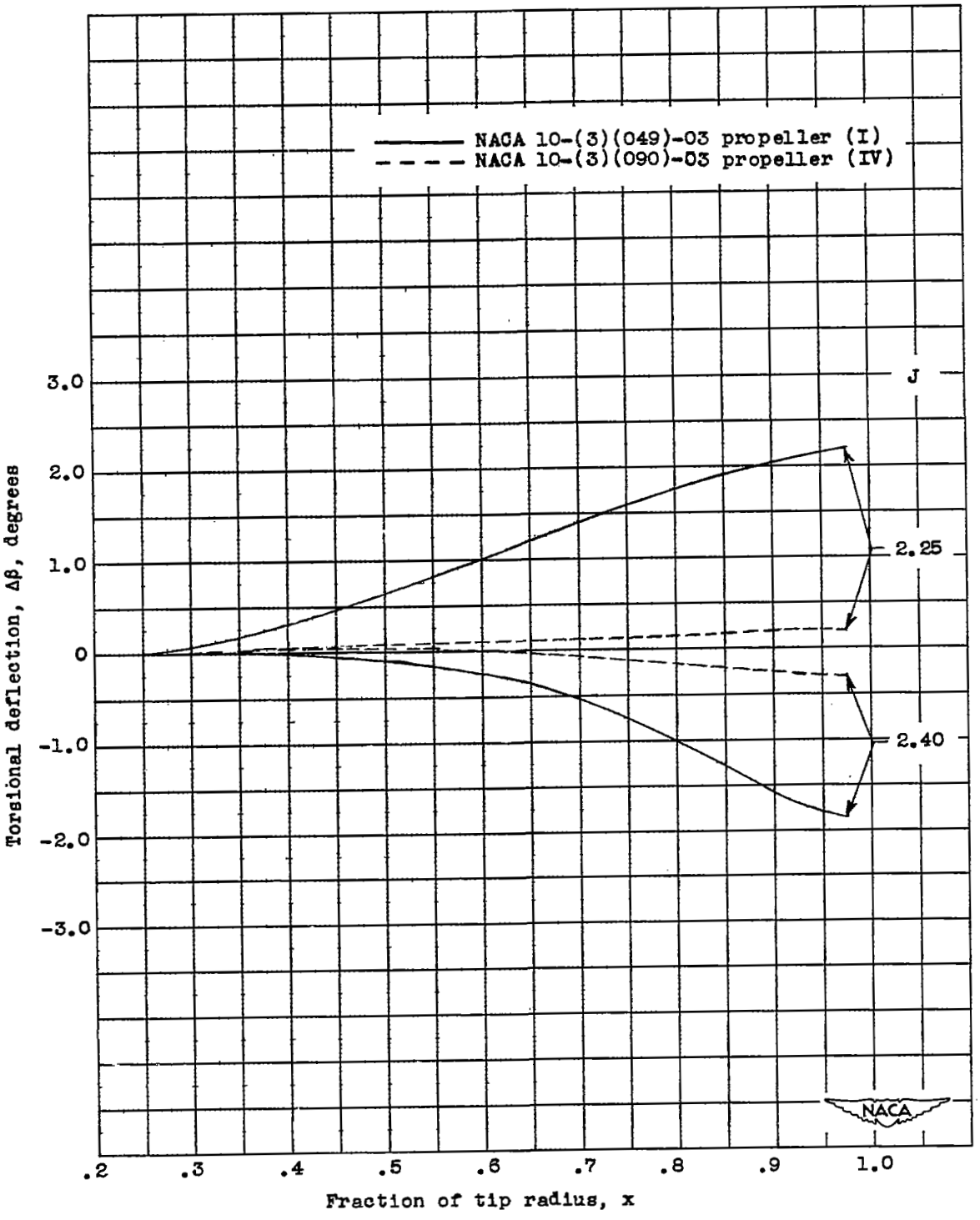

Figure 9.- Relative magnitude of torsional deflection for blades differing only in thickness. 1600 rpm; $\beta_{0.75R} = 45.0^{\circ}$.

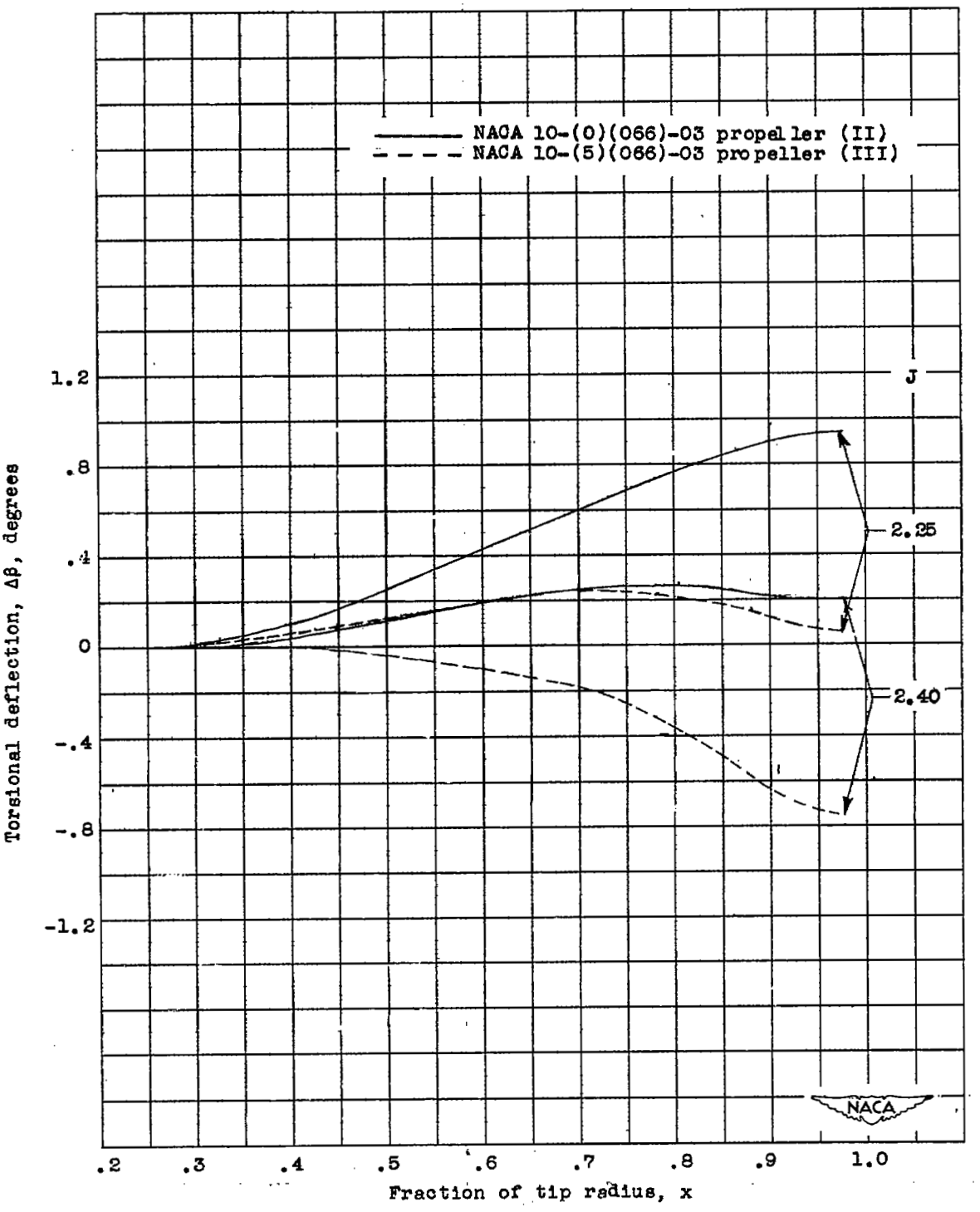

Figure 10.- Relative magnitude of torsional deflection for blades differing only in camber. 1600 rpm; $\beta_{0.75R}$ = 45.2° (II); 45.0° (III).

[redacted]

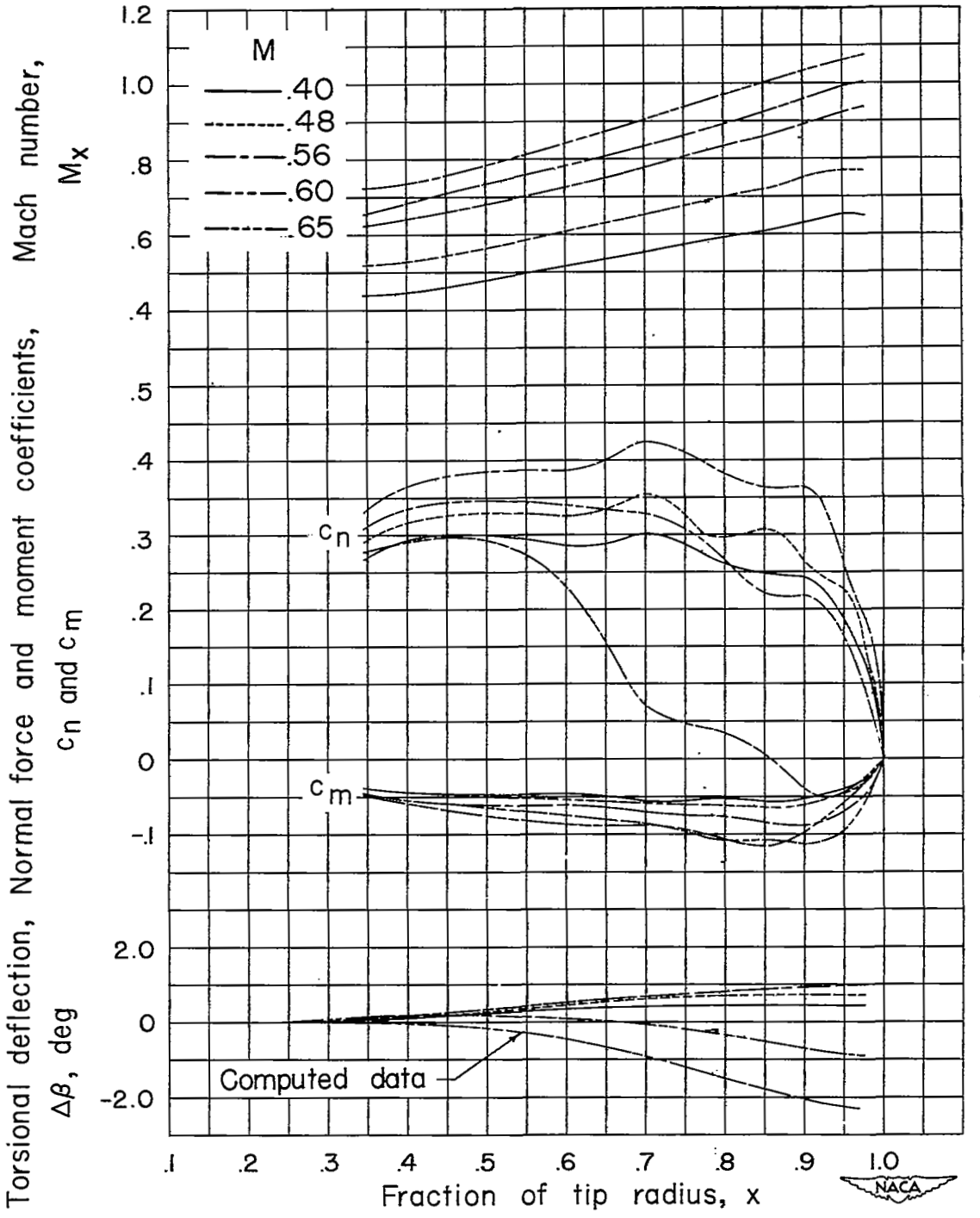

Figure 11.- Effect of Mach number on loading and resulting torsional deflection. NACA 10-(3)(049)-03 propeller (I); $J = 2.30$; $\beta_{0.75R} = 45.0^\circ$.

[redacted]

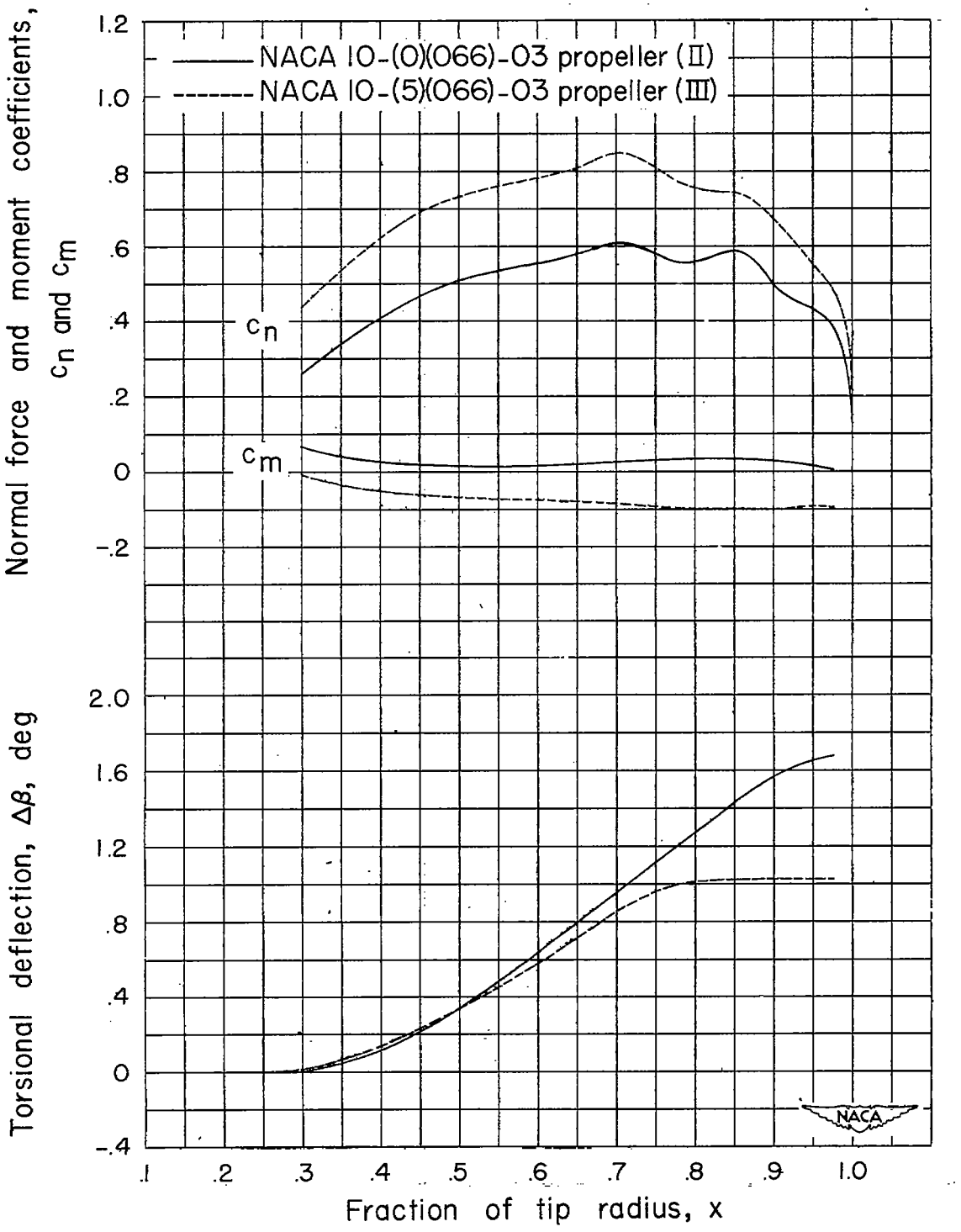

Figure 12.- Effect of normal-force and moment coefficients on torsional deflection. 1500 rpm; $J = 2.00$; $\beta_{0.75R} = 45.2^\circ$ (II); 45.0° (III).

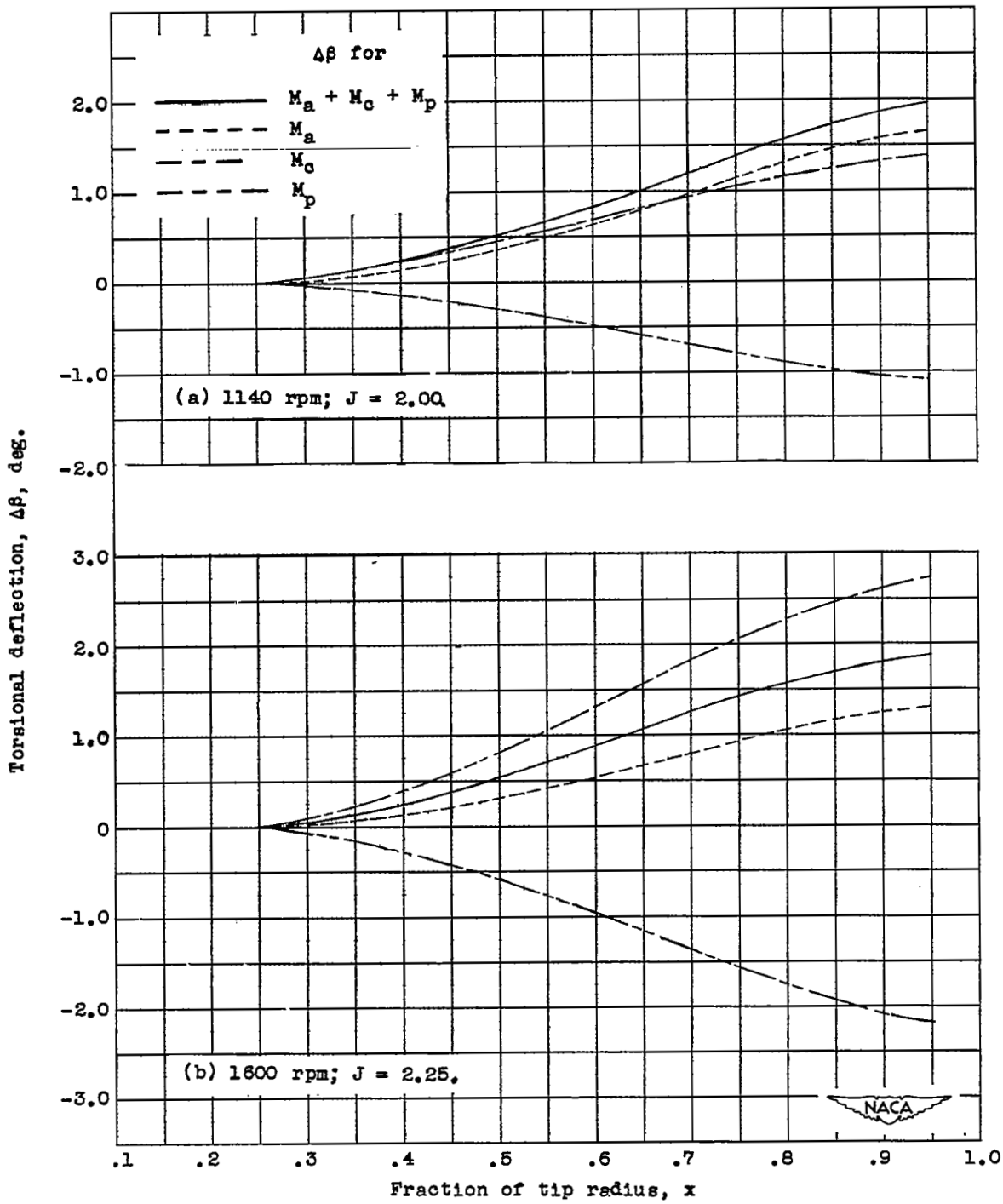

Figure 13.- Operating factors contributing to blade twist. NACA 10-(3)(049)-03 propeller (I); $\beta_{0.75R} = 45.0^{\circ}$.

[redacted]

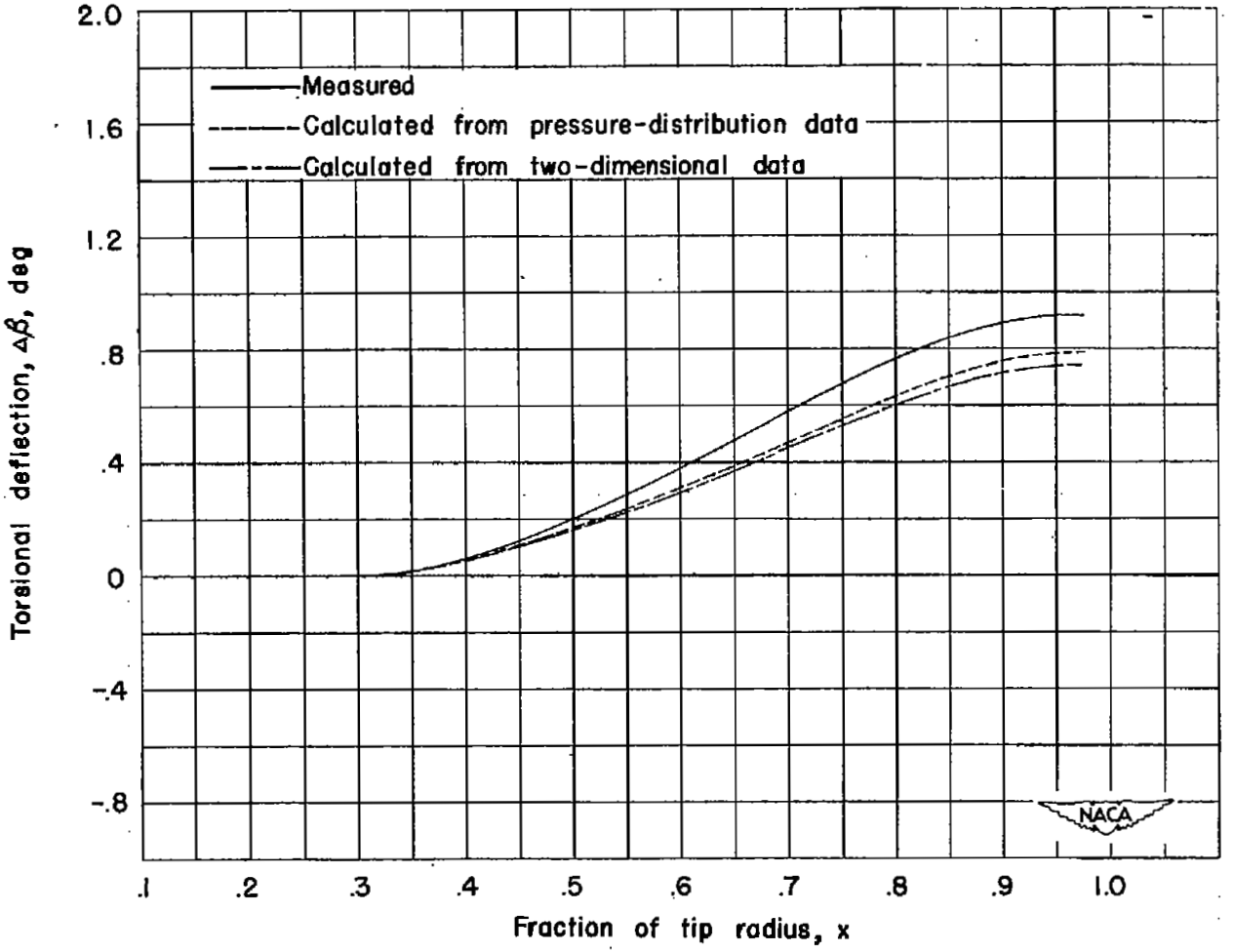

Figure 14.- Comparison of measured blade twist with values calculated using pressure-distribution data and two-dimensional data. NACA 10-(5)(066)-03 propeller (III); 1140 rpm; J = 1.80; $\beta_{0.75R} = 45.0^{\circ}$.

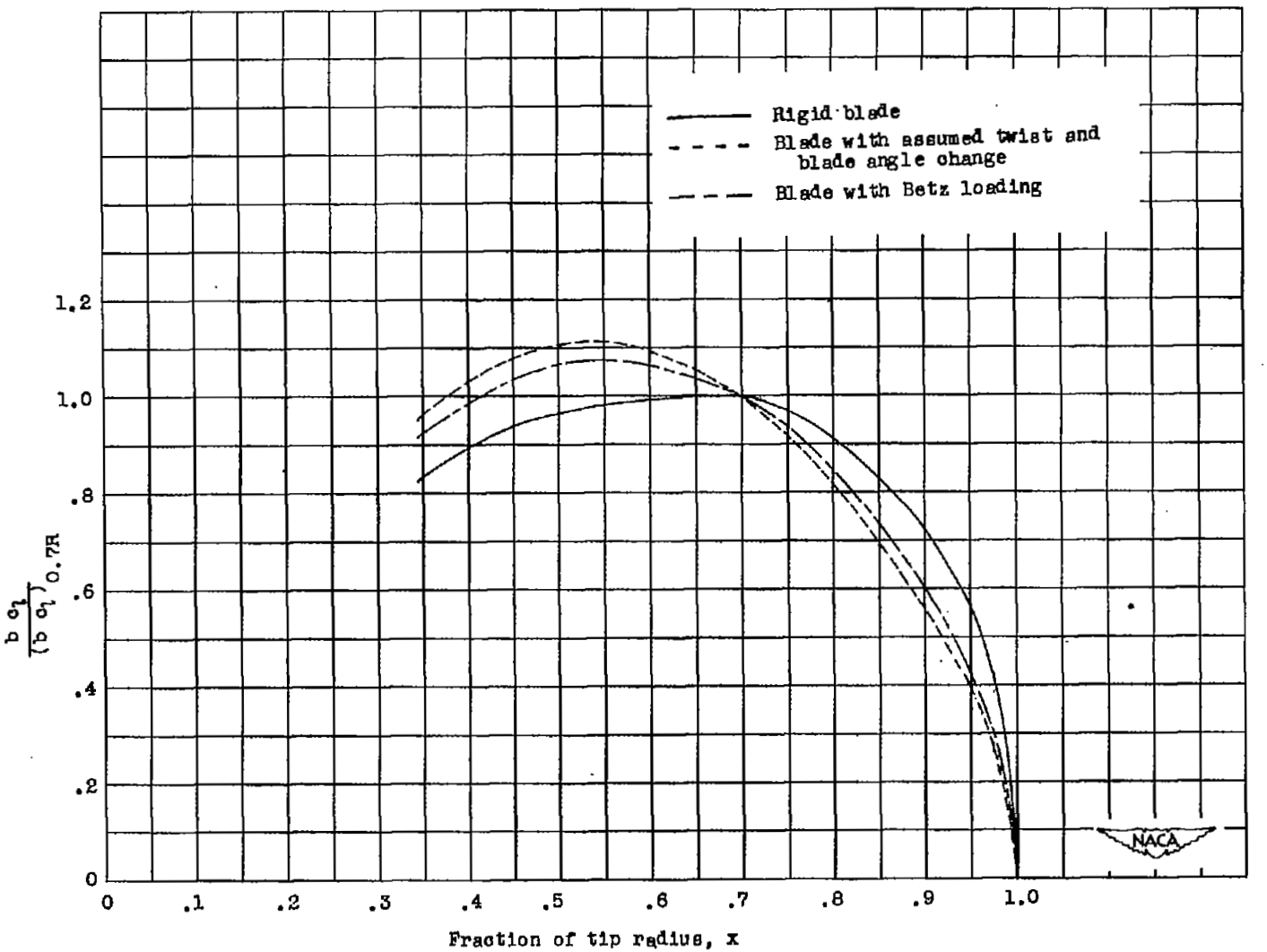

Figure 15.- Effect of blade twist on blade loading. NACA 10-(3)(049)-03 propeller (I); M = 0.60; J = 2.25; $\beta_{0.75R} = 45.0^{\circ}$.

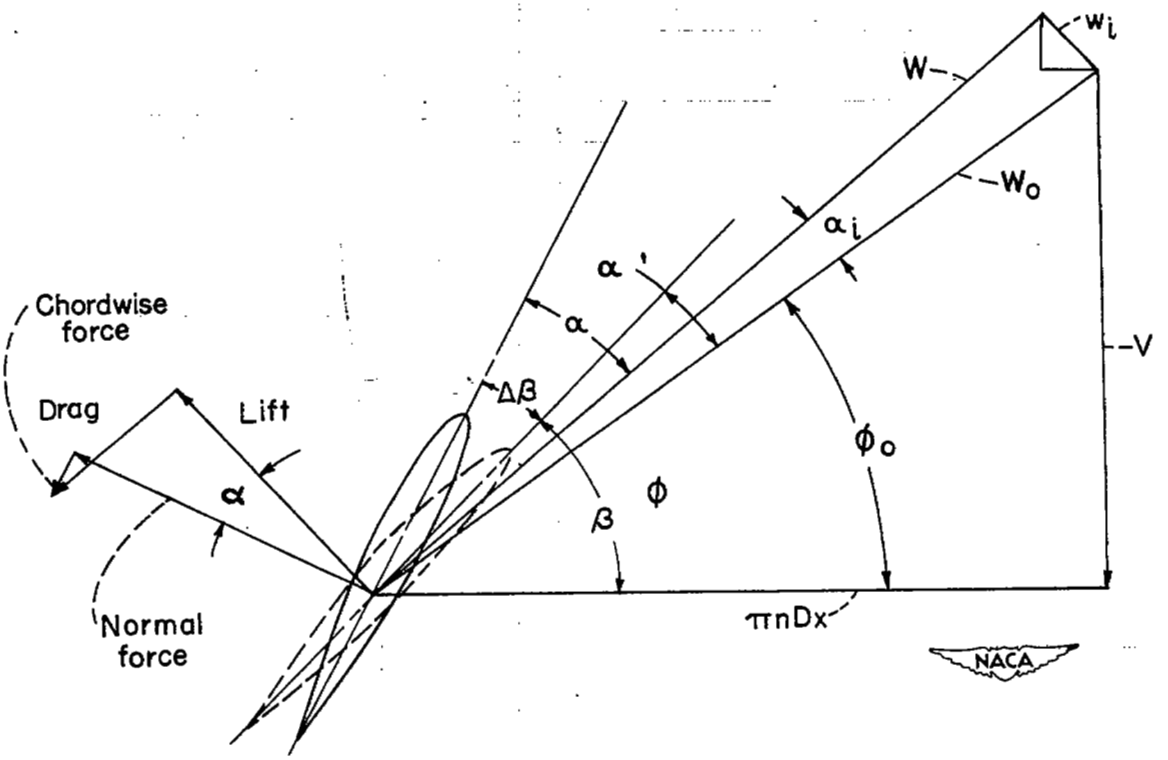

Figure 16.- Vector diagram of the velocities and forces acting on a blade section.

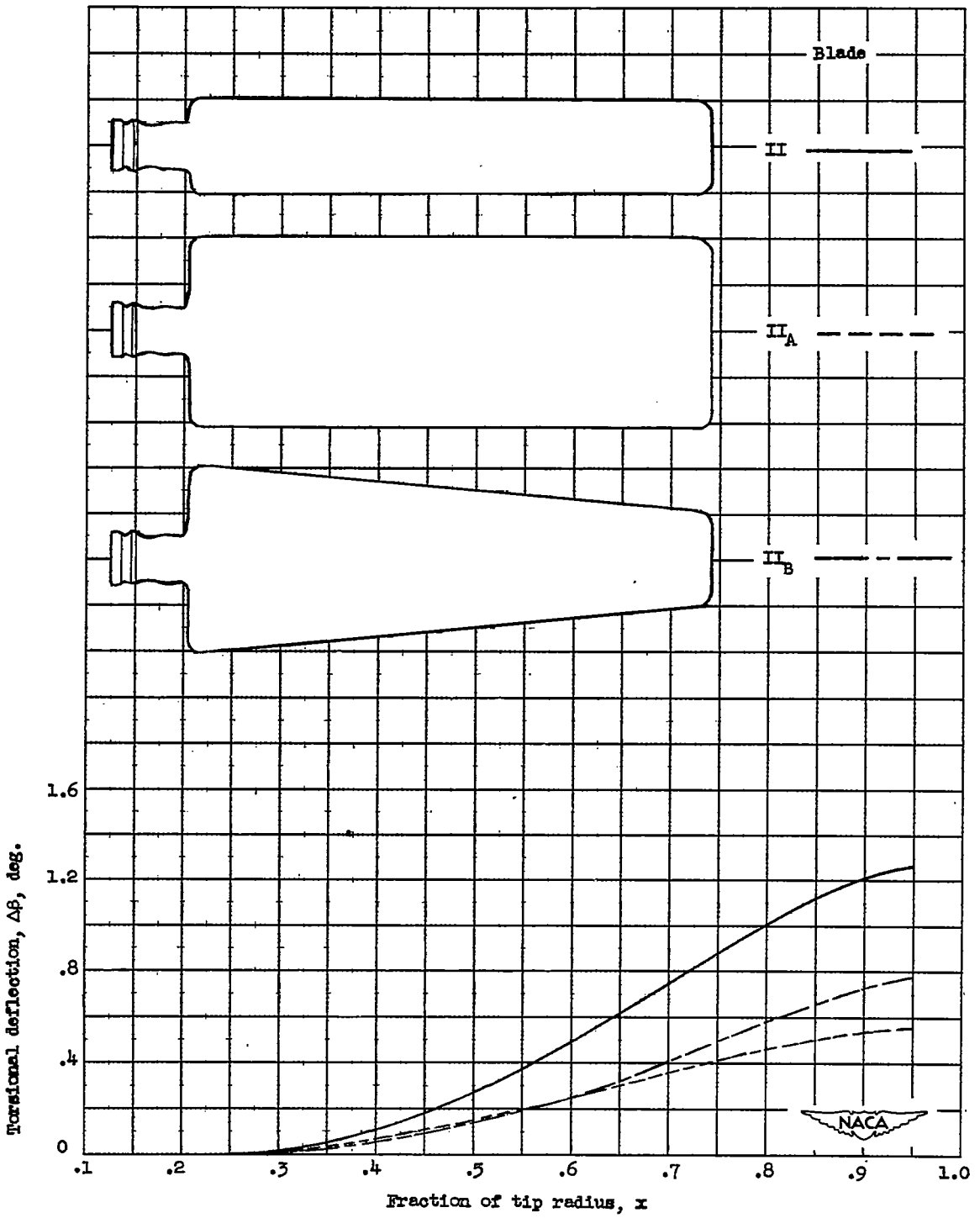

Figure 17.- Effect of plan form on blade twist. 1600 rpm; J = 2.20; $\beta_{0.75R} = 45.2^{\circ}$.

[redacted]

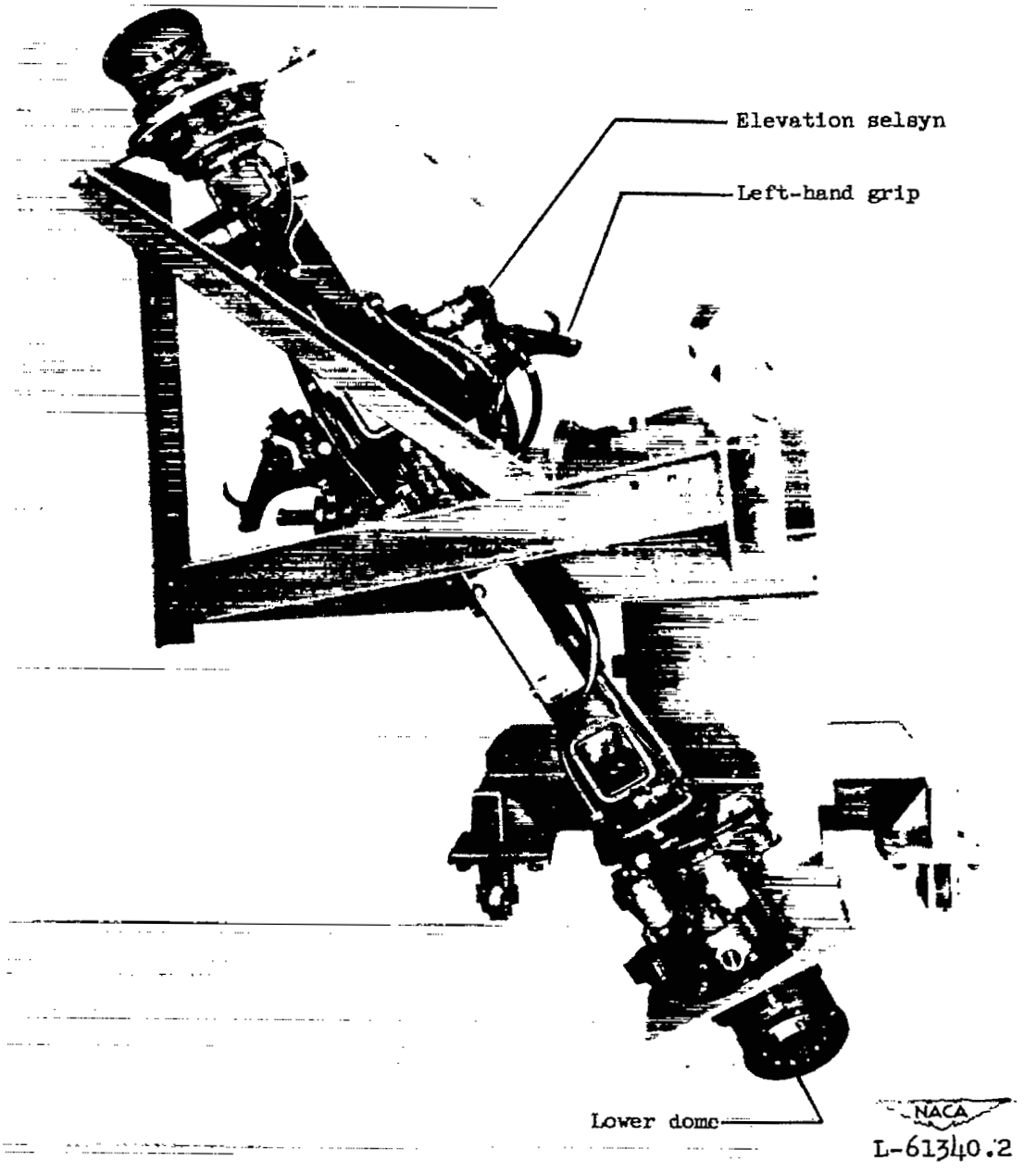

Figure 18.- Photograph of optical deflectometer.

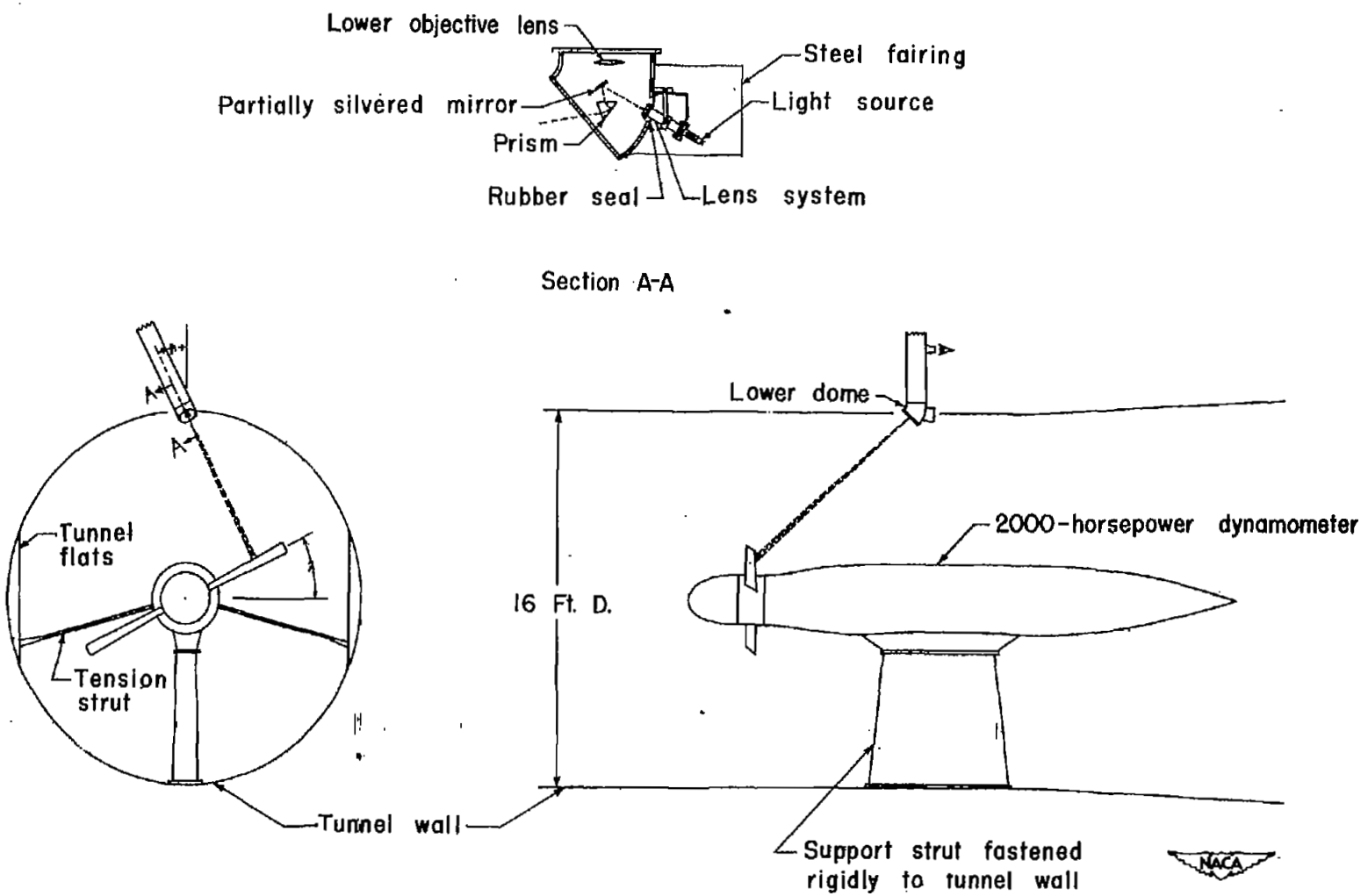

Figure 19.- Diagram of apparatus.

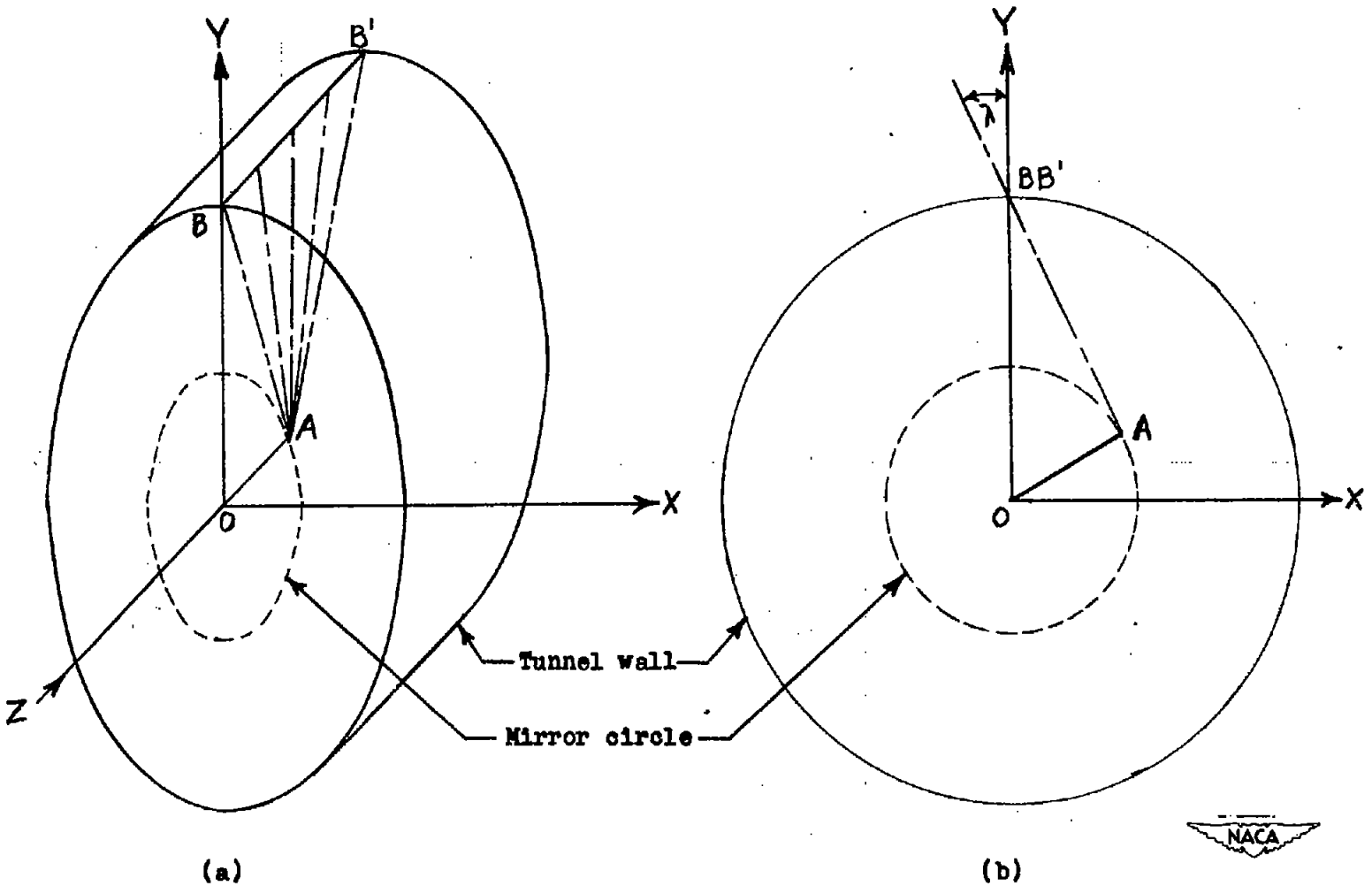

Figure 20.- Geometry of optical path.

NACA-Langley - 6-22-51 - 375